1991

Three-dimensional predictions of incipient fluidization in fine sands in unbounded domains, 80p. (no date but assume 1991)

Gerard P. Lennon

William MacNair

THREE-DIMENSIONAL PREDICTIONS OF INCIPIENT FLUIDIZATION IN FINE SANDS IN UNBOUNDED DOMAINS

by

Gerard P. Lennon and William MacNair

Lehigh University

Bethlehem, PA 18015

IMBT HYDRAULICS LAB REPORT # IHL-132-91

TABLE OF CONTENTS

LIST OF TABLES

LIST OF FIGURES

LIST OF FIGURES

LIST OF FIGURES

ABSTRACT

Fluidization systems in the coastal environment can be used to maintain a channel as an alternative to dredging. These systems consist of a water pumping system and a source pipe with perforations at or near a tidal inlet. Fluidization studies have been conducted at Lehigh University over the past several decades. Previous work has included laboratory pilot scale testing to gather pressure vs. location data and mathematical model studies using two-dimensional finite difference and finite element methods. This work evaluates the three-dimensional effects of fluidization using the finite difference model developed by McDonald and Harbaugh (1988) (herein after referred to as the "MODFLOW Model"). The flow is mostly two-dimensional, being uniform along the pipe except for variations close to the pipe caused by the fact that there are small holes (usually 1/8" diameter) spaced 2 inches apart.

The major conclusions of this study are:

- a highly refined grid near the source pipe holes is required because this is where the greatest change in head occurs. This had already been determined in the 2-D studies and it was shown to be even more critical in the 3-D models. The greatest change in head occurs at the nodes adjacent to the source perforation constant head nodes. The distance between nodes at these locations had to be reduced to extremely small dimensions to achieve an evenly spaced head distribution over the entire model.

- three-dimensional effects become negligible at locations further than about four centimeters away from the fluidization source pipe holes. A significant amount of head is lost in the immediate vicinity of the holes.

- for a given pipe pressure, the overall difference in hydraulic head predicted using a 2-D (vertical profile) grid ranges from about four times the 3-D grid model near the source to about double the 3-D model at locations further away from the source pipe area, resulting in a lower flowrate for this pipe pressure.

- for a given pipe pressure, the high losses near the source holes results in the hydraulic head in the 3-D model being a factor of 2-4 times less than the 2-D results far from the pipe, resulting in a much lower simulated flow rate. By setting a higher head at the pipe holes to overcome this loss, a head distribution can be selected that is the same for 2-D and 3-D simulations except for the region within four centimeters of the pipe. The resulting 3-D vertical gradient prediction is then virtually the same as the 2-D gradient prediction, resulting in the same velocity field, and the same incipient flow rate.

CHAPTER 1 - INTRODUCTION

Fluidization is the upward flow of a fluid through a granular bed of particles at sufficient velocity to suspend the grains in the fluid. Fluidization occurs when there is sufficient fluid flow to exert an upward drag on the particles equal to their submerged weight. For fluidization to occur, the hydraulic gradient must be slightly greater than unity in the upward direction.

Fluidization studies using fine sands have been conducted at Lehigh University over the last several decades examining pre-, incipient and post-fluidization. This work is a continuation of those studies using a three-dimensional finite difference ground water flow model (McDonald and Harbaugh,1988). The current work evaluates the construction of model matrices and layers (slices) to evaluate 3-D effects. These will be compared to 2-D studies conducted by Lindley and Lennon(1991) and 2-D finite element studies conducted by Kopaskie(1991).

1.1 Incipient Fluidization

The theory of fluidization is discussed by, among others, Bear (1972), Weisman et al (1988), Roberts et al (1986) and Kopaskie (1991). Fluidization can best be described as the upward flow of a fluid through a granular bed at sufficient velocity to suspend the grains in the fluid (Cleasby and Fan, 1981). Flow through orifices in a source pipe can fluidize a region in the media above the source pipe. Clifford (1989) identified five distinct processes: pre-fluidization, initiation of fluidization (incipient fluidization), full fluidization

where a region of the sand bed above the source pipe is expanded, slurry removal from the fluidized region, and erosion of the remaining sand bed by the jets once the slurry is removed. This study is primarily concerned with the initiation of fluidization or incipient fluidization. The minimum vertical velocity, V_y, causing fluidization is determined from the upward flux rate given by Darcy's Law:

$$V_y = K_y J_y$$

Where

K_y = hydraulic conductivity in the vertical direction

J_y = the negative hydraulic gradient.

The critical hydraulic gradient to produce incipient fluidization is generally considered to be unity (Bear, 1972). The hydraulic heads determined in this three-dimensional study will be used later to determine hydraulic gradients to show where incipient fluidization should occur in a physical model. This then would later be verified using an appropriate physical model.

1.2 Finite Difference Simulation of Incipient Fluidization

The finite difference model used here is the McDonald and Harbaugh (1988) modular groundwater flow model (MODFLOW Model). This model was developed based on the theoretical development presented in Chapter 2 of the MODFLOW Model documentation. Equation 1 of McDonald and Harbaugh (1988) is the general partial differential equation describing ground water flow:

$$\frac{\partial}{\partial x}\left(K_{xx}\frac{\partial h}{\partial x}\right)+\frac{\partial}{\partial y}\left(K_{yy}\frac{\partial h}{\partial y}\right)+\frac{\partial}{\partial z}\left(K_{zz}\frac{\partial h}{\partial z}\right)-W=S_s\frac{\partial h}{\partial t}$$

where

x, y, and z are Cartesian coordinates aligned along the major axes of hydraulic conductivity, K_{xx}, K_{yy}, K_{zz};

h is the potentiometric head (L);

W is a volumetric flux per unit volume and represents sources and/or sinks of water (t^{-1});

S_S is the specific storage of the porous material (L^{-1}); and

t is time (t).

This equation is combined with Darcy's Law and the continuity equation to yield an equation for hydraulic head (Equation 26 of McDonald and Harbaugh, 1988).The development of finite difference equations is described by many sources such as Freeze and Cherry (1979).The experimental conditions can be simulated by using these equations along with the appropriate boundary conditions.

In this study, the numerical model is used to simulate conditions in a physical model that has been run to obtain actual pressure data. This physical model is located in the Imbt Hydraulics Laboratory at Lehigh University. Figure 1.1 is a side view of the physical model. The model is filled with fine sand and is 360 cm. long by 102 cm. deep by 30.5 cm. wide. The width is narrow enough to consider this model as essentially a 2-dimensional model, which is what has been done in previous studies. This study, however, does consider the 3-D effects. Figure 1.2 shows the third dimension of the model. This end view shows detail of the fluidization pipe

which has 0.317 cm. orifices spaced every 5.08 cm along the width of the tank. A constant hydraulic head is supplied to these perforations to supply the fluidization force. In the 2-D studies, these orifices are essentially modeled as a "slot" along the width of the tank since there is no way of varying conditions along this third dimension, where as the 3-D model represents these holes spaced 2 inches apart. Figure 1.3 shows the data acquisition system of the physical model. The pressure readings obtained from this system give a way of validating the results obtained in the 2-D and 3-D numerical studies.

1.3 Scope of Study

The scope of this work is to extend the basic 2-D MODFLOW Model grid developed by Lindley and Lennon (1991) to three dimensions. The model was run on the Lehigh University Sun Unix computer system. The 2-D Model used a single, uniform, "vertical slice" to simulate the physical system. The third dimension, i.e. the width of the system, was modeled by adding another slice (or "layer" according to MODFLOW documentation) to the simulation. Subsequently, additional "slices" were added to form 3, 4, 5, 6, and 7 vertical slices (layers) successively to evaluate how the head variation changed as the model was divided into more layers. McDonald and Harbaugh (1988) intended the user to view these layers as "horizontal slabs". However, for this application, they are used as vertical slices. The term "layer" in the McDonald and Harbaugh MODFLOW documentation corresponds to the term "vertical slice" in this study.

After a 5 vertical slice simulation was run, a grid sensitivity evaluation was made to determine how the layer spacing should be chosen to reduce the computational error. Two criteria are used to judge the computational error. The major criterion is to choose the grid spacing in all three directions to minimize the maximum change in head in any cell to an adjacent cell in the grid. The other criterion is to have a change in head evenly distributed over the nodes. Even though the grid resolution was chosen to be very fine near the source holes, the largest change in head occurs between nodes in the immediate vicinity of the source holes. Additional studies were completed with 6 and 7 vertical slices, first changing most of the slice thicknesses and then changing the row and column distribution in the horizontal and vertical directions.

CHAPTER 2 - APPLICATION OF THE FINITE DIFFERENCE MODEL

2.1 Description of Domain Being Simulated

Figure 2.1 shows a definitional sketch of 2 dimensions (a vertical slice) of the physical model simulated by the MODFLOW model. This slice is a portion of the model that includes perforations supplying the constant hydraulic head that causes fluidization of the sand bed. In the 3-D numerical simulation, some of the slices contain these holes and some do not. Figure 2.2 is a top view of this model showing the third dimensional area being modeled. This particular view shows the dimensions for the 5-layer model run. The upper diagram in this figure shows the entire physical model with the portion that was modeled numerically in crosshatch. The lower plot in this figure shows an exploded view of the crosshatch area.

These two figures allow a discussion of the boundary conditions that are used in the simulations performed in this study. At the sand surface h is set to zero. On the impermeable side walls the gradient is zero ($\partial h/\partial x=0$), as is the case along the impermeable bottom ($\partial h/\partial y=0$). Since Darcy's Law is the product of gradient and hydraulic conductivity, a zero gradient results in an impermeable boundary. Along the solid source pipe, $\partial h/\partial n$, the head gradient in the normal direction, is also zero, representing an impermeable (no flow) boundary except for the orifices which have a boundary condition of specified head, simulating flow. There is also a symmetry boundary along the vertical plane that bisects the source pipe. In the 3-dimensional simulations done in this study, an additional no flow boundary is specified at the point of

symmetry located on a vertical plane situated one half way between two source holes.

2.2 Selection of a Model

Table 2.1 summarizes the three modeling efforts applied to fluidization to date. MODFLOW is selected as the model to use for continuing study. Its versatility in modeling a range of sites, its acceptability and straightforward use make it the best choice of those considered. Its versatility should make MODFLOW a strong candidate for use in any future fluidization studies.

2.3 Description of MODFLOW Model Components (Packages)

The Modular 3-Dimensional Finite-Difference Groundwater Flow Model (MODFLOW), McDonald and Harbaugh, 1988, has the capability to simulate transient 1-, 2- and 3-dimensional groundwater flow in an inhomogeneous and anisotropic aquifer system of multiple layers. This model uses a rectangular, block centered, finite-difference calculation and allows for a variable grid. Layers can be defined as either confined or unconfined.

The computer program is designed to operate through highly independent modules organized into "packages". These modules allow the user to incorporate stress from pumping or injection wells, areal recharge, flow-through river beds, drains, evapotranspiration and general head boundaries.

Representation of special features such as vertical barriers can be affected in the MODFLOW code through mathematical manipulation of conductivities

and grid dimensions through use of the equations described by Hansen (1991).

Differences in the third dimension can be represented by changing properties in different layers(vertical slices). For example, alternating layers of clays and sands can be depicted by assigning different transmissivities to the different layers. In this fluidization simulation, the slices with perforations are represented by including a constant hydraulic head of 100 cm.

The model output contains an extremely large number of data points. The 69 row by 74 column by 7 vertical slice model contains 35,742 output points. In order to confine the data analysis to a manageable number of points, the UNIX operating system language was used to "cut" important rows or columns out of the output. UNIX programs and files were used or created to accomplish this. Lotus/Excel programs were used to plot results downloaded from the Lehigh SUN minicomputer system.

2.4 Description of key MODFLOW Inputs for this study

The computer package inputs used to run the MODFLOW Models evaluated here are listed and described in Table 2.2. The MODFLOW Model documentation was used to specify input for this program. This documentation gives very specific instructions on how the input parameters must be specified. The key input packages used for each simulation are the ".BAS" and the ".BCF" packages. The .BAS package is the "Basic" input file while the .BCF package is called the Block Centered Flow Program.

.BAS Package Input

The .BAS input includes the files used for input and output as well as a description of the matrices used. This study uses a 74 column by 64 row matrix in all cases. Initially, in the two slice model system, both slices contained a 100 cm constant hydraulic head to simulate the head supplied by the source pipe. This was done to validate the 3-D model vs. the previous 2-D model study. After this comparison was verified, one slice was changed from the 100 cm hydraulic head to impermeable where there was no perforation or orifice in the source pipe. This more accurately portrays the actual physical model which had a hole spacing of 5.08 cm (2"). The 2-D model was actually simulating the head from a slot along the pipe rather than 1/8" holes spaced every 2". All other hydraulic head values were determined by the model or were boundaries on either model edges or surface conditions. A separate input matrix must be added for each slice (layer).

.BCF Package Input

The .BCF input includes the spacing of the rows and columns as well as the hydraulic transmissivity and the hydraulic conductance between slices. Aside from the general matrix dimensions and initial boundary conditions which are input in the .BAS input, this file contains all critical spacing and hydraulic parameters.

The key hydraulic parameters that are input are the transmissivity and conductance. Both are a function of the hydraulic conductivity, K. The K for the sand used in this model has been determined by others using several

methods. The K value used in this study was 0.012 cm/sec. The transmissivity is calculated as follows:

T = K x thickness of layer(slice).

A separate transmissivity is input for each slice in the model.

The hydraulic conductance, C, is calculated according to:

$$C = \frac{K}{\text{Length between nodes of 2 layers(slices)}}$$

Conductance is used to calculate the flow between layers and there will be one less conductance value than layers, i.e. the last layer does not have to conduct water between it and the edge of the model and therefore no conductance value is input for that layer.

CHAPTER 3 - MODEL TRIAL DISCUSSION

3.1 Summary of Simulations

The starting point for the simulations used in this study was the one vertical slice model developed by Lindley and Lennon (1991). The side view of the model was shown in Figure 2.1.. The single vertical slice model is homogeneous through the "z" direction (perpendicular to the page). Figure 3.1 is a side view of the model showing the finite difference grid in the x-y plane. There is a very fine grid dimension around the source hole because this is where the greatest amount of change in head occurs over extremely small distances. Figure 3.2 is an enlarged view of the finite difference grid around the source hole. Figure 3.3 is a further enlargement of the grid in the source hole area. This grid is similar to that of Lindley and Lennon (1991), which was used in all model runs of 5 slices or less. Towards the end of this simulation study, the finite difference grid was modified to what is shown in these figures to obtain a more uniform change in head between nodes. The modifications made an even finer grid at the source hole boundaries. The differences between the two finite difference grids can be seen in Tables 3.1 and 3.2, which show the column and row spacings, respectively. These spacings are input into the "block centered flow" or .BCF package.

Two identical vertical slices were used to start the multi-layer study. The two identical slices were then changed to one slice with a constant head of 100 cm. representing the fluidization perforation and one slice with a constant head of zero to represent the solid pipe surface. Then a progression of simulations was completed adding one slice each run as shown in Figure

3.4. Simulation No. 1 contained two identical slices, both with the 100 cm. constant head, which represents a perforation (actually a slot in the 2-D case) across both slices. Simulation No. 2 simulated the perforation in one slice with a hydraulic head of 100 cm, and no perforation in the second slice, which was simulated with a no-flow node in the matrix. Simulation No. 3 included one slice with the perforation and two slices without the perforation. The four slice run (Fig. 3.4, Simulation No. 4) included two slices with and two without the perforation, while the five slice run (Fig. 3.4, Simulation No. 5) included two with the perforation and three without. After these simulations were completed, an evaluation of the change in head between slices was made and it was decided to add a sixth slice along with varying the thicknesses of the slices without the perforation (Figure 3.4, Simulation No. 6). Then an additional six slice run was made, changing the spacing of the rows and columns in the .BCF file. This change in spacing of rows and columns was also done with the objective of obtaining a similar head change between successive rows and columns. A seventh slice was added to optimize the change in head between slices. A second seven slice run was completed to achieve a more even change in head between successive slices. The dimensions of the slices in these 7 slice simulations are shown in Figure 3.4, Simulations 7a and 7b. Finally, a 2-D, 2 slice model was run with the "slot" size reduced to have equivalent area to the holes in the multi-slice runs. This run was used to compare the 2-D model results vs. the 3-D model.

3.2 Discussion of Results

The results of these model runs are shown pictorially in Figures 3.5 through 3.31. Figures 3.5 through 3.15 show cross sections along the length of the model using Row 38 which is opposite the center of the hole or perforation supplying the 100 cm. constant hydraulic head. This row is considered the most useful row to show the variation in head with distance from the source. Figures 3.16 through 3.26 show the variation of head in a cross sectional view at Column 25. This column is also considered a key column to show the variation of head in three dimensions because the column crosses the source pipe in front of the hole.

The results of running the two through five slice cases showed some inconsistencies in how head varied as an additional slice was added to the model. This could have been caused by the fact that as one slice was added, the thickness of other slices were changed, i.e., more than one change was made to the model with each progressive run. In addition, the change of heads between slices was not equal and it was decided to alter the distribution of thickness of the slices in the six slice runs. Also, there were large changes in head near the source as shown on data gaps in the Column 25 cross sections that show the entire head profile from 0-100 cm. It was decided to change the row and column spacings in the .BCF file. The revised vs. original .bcf column/row spacings are shown in Tables 3.1 and 3.2. These six slice runs are shown in Figures 3.11, 3.12, 3.22 and 3.23. There was a large improvement in the distribution of head with the new spacing between the rows along columns. This can be seen by comparing Figure 3.22 to Figure 3.23. All model plots were produced using Excel and where

comparisons are discussed they are in similar scales so that similarities and differences are clear.

Further optimization was obtained by running 7-slice simulations. Both 7-slice runs used the revised .BCF spacing for rows and columns. The slice thicknesses were adjusted as shown in Figure 3.4, Simulation No. 7a and 7b. The resulting head distributions are plotted in Figures 3.13 through 3.15 for Row 38 and Figures 3.24 through 3.26 for Column 25.

The final 7-slice simulation shown in Figures 3.4-Simulation No. 7b, 3.14, 3.15, 3.25, 3.25A and 3.26 was considered the optimum for this study. Figure 3.27 is a "ribbon plot" of this 7-slice model run. This figure gives an alternate view to show how the change in head is distributed over the 7 slices. Examination of this figure shows that the change in head between slices is much more even in the middle slices. There were other competing factors that prevented obtaining a more even distribution at the slices near the edges. At the perforation, which was located in slices numbered 1 and 2, the change in head between slices was small. There was a large change between slices 2 and 3, which is where the transition from a slice with the constant head (perforation) meets a slice without the constant head. This large change was minimized in successive simulations by making these 2 slices smaller. In the final 7-slice simulation, the thickness of slice 2 was only 0.04 cm. and slice 3 was only 0.02 cm. The distance between nodes of adjacent finite difference cells located on these 2 slices was only 0.03 cm. There was also a smaller change in head at the outer slices numbered 6 and 7. Despite this small change in head, the size of slice number 7 was not increased because it was already substantially wider than any other layer - 1.5 cm. vs.

0.6 cm. for slice 6, which is the next largest slice. It was felt that making this layer wider would compromise some of the model calculations, or, in other words, making this already large slice bigger would concentrate the calculations into a thickness that would be a very small percentage of the total thickness.

Examination of the figures comparing the heads calculated using the initial two identical slices and those calculated in any of the models using one or more slices with no flow nodes shows that the two identical slice model results in a calculated head that is 2-4 times the results of the models with no flow slices. The identical slice model is really simulating a "slot" across the entire model thickness, rather than a perforation. To determine if the additional perforation area added by this simplified simulation was what was causing the higher resulting heads, an additional 2-slice simulation was run with a slot size reduced to the equivalent area of a perforation. The results of this simulation, shown in Figures 3.28 through 3.31, show that the estimated head is still higher than simulations run with no flow slices. No additional study to determine the cause of this phenomenon was completed.

3.3 Vertical Gradient Calculations

A key objective of this study was to calculate the vertical hydraulic gradient, J, and compare the 3-D results to the 2-D results determined previously by others. Figure 3.32 shows the results of the calculations in a plot of elevation vs. vertical gradient. The plots are shown at locations at the center of the source pipe (x=0), at the source hole (x=2.54), and at a point 9

cm. away from the center of the source pipe. The calculated gradients are essentially the same for all slices and are very similar to the previous 2-D results. Apparently, while the 3-D calculations showed some difference in head between slices, the vertical gradient within any slice is very similar to the other slices because the calculation is based on a region above the region of significant 3-D effects.

The calculations for determining J are shown in Table 3.3, an Excel spreadsheet. The key calculations are summarized as follows. The difference in head between any two nodes is simply the subtraction of the two heads calculated by the MOD Model at those two points. The distance between two nodes is the distance between the center points of those two nodes. After these "raw" gradients are calculated, a factor is developed to multiply all gradients so that the overall average gradient is 1.02, which is the necessary gradient for fluidization according to theory. This factor was determined by calculating the average gradient for the 15 cells located above the pipe at a distance of approximately 9 cm. from the pipe. Column 62 in the matrix is located about 9 cm. from the pipe. After this average "raw" gradient was calculated, it was divided into 1.02 to determine the correction factor. The factor determined by these calculations was 3.89. All "raw" gradients were multiplied by this factor. The gradients calculated with the hydraulic heads from the MODFLOW model would have been the same as these adjusted gradients if the initial constant head used for the source pipe was 389 cm. rather than 100cm.

Table 3.4 shows calculated gradients (J) at "key" locations. The locations considered important for comparison were at the source pipe center line, at

the source perforation, and at a point 9 cm. away from the pipe center. The multi-layer calculations are identical directly over the pipe and at 9 cm away from the pipe, so that only one value is shown. Calculated gradients at the source perforation are shown for the first, third and seventh slices. The gradients at the source pipe center line, the source hole and at 9 cm. away from the pipe center are plotted on Figure 3.32. While there is some difference in the values calculated at the source hole for the three slices, it is not visible on the scale plotted in Figure 3.32. Finite element calculations (Kopaskie 1991) are shown for comparison. A comparison with the finite element calculations using a larger scale is shown in Figure 3.33. The gradients calculated using the two methods for a 9 cm distance from the pipe are similar. Lennon et al (1991) provide comparisons to experimental data.

3.4 Hydraulic Head Predictions

The MODFLOW predicted hydraulic head is shown in Figure 3.34. The water flow is perpendicular to the lines of equivalent hydraulic head. Near the source hole, the flow is generally upward, although there is some horizontal and downward flow component. The hydraulic head plots are similar to the two dimensional studies, even though the calculated head is lower than the head calculated in the 2-D studies.

CHAPTER 4 - CONCLUSIONS AND RECOMMENDATIONS

4.1 Conclusions

The first key conclusion from this work is that the three-dimensional effects disappear after about four centimeters distance from the perforation. This fact is important because it can be used to evaluate what weaknesses there are in two-dimensional models run which are more widely available and are easier to input and run than a three-dimensional model. The second major conclusion is that the overall head predicted by the three-dimensional model varies from about one fourth the single layer model near the source to about one half the single layer model at locations further away from the source. This factor is also important when comparing 2-D models to real three-dimensional effects. In addition, it was found to be important to review the spacing of layers, rows and columns to try and get an equal change in head between each layer. This was not always possible. The key area of change is the location where the perforation meets the solid pipe and there are several layers focused in this area to simulate the head change around these perforations.

4.2 Recommendations for Future Work

The following is a list of suggested tasks that would enable further verification of the mathematical models being used to predict fluidization. These further verification studies would help to make the models more valuable as predictive design tool in the development of fluidization systems.

For the physical model, test the validity of the 3-D model studied herein by placing multiple pressure probes along the thickness of the model at points close to the source pipe. For the MODFLOW numerical model, vary the "Strongly Implicit Procedure" (SIP) parameters to assure that the solutions determined here are accurate. The closure criteria resulted in errors ranging from 0.5% for the two slice simulations up to 8.75% for the seven slice runs. While these errors are high, the results obtained as the number of layers was increased appear consistent. Using additional iterations should eliminate this problem. A refinement of the grid should be conducted by adding additional layers.

TABLES

TABLE 2.1
COMPARISON OF THIS STUDY VS. PREVIOUS INVESTIGATIONS
APPLICATION OF CONSIDERED MODELS

	FEM KOPASKIE (1991)	2-D MODFLOW LINDLEY (1991)	3-D MODFLOW (THIS INVES-TIGATION)	FUTURE SUGGES-TIONS
PUBLIC DOMAIN	NO	YES	YES	YES
IRREGULAR GRID	YES	YES	YES	YES
DIMENSION SIMULATED	2-D	2-D	3-D	3-D
CAPAPBLE OF TRANS-IENT	NO	YES	YES	YES
SIMULA-TION STEADY OR TRANSIENT	S	S	S	T

FEM - FINITE ELEMENT METHOD

TABLE 2.2 - LIST OF PACKAGES

PACKAGE NAME	ABBREVIATION	PACKAGE DESCRIPTION
Basic	BAS	Handles those tasks that are a part of the model as a whole. Among those tasks are specification of boundaries, determination of time, step length, establishment of initial conditions and printing of results.
Block centered flow	BCF	Calculates terms of finite difference equations which represent flow within the porous medium; specifically, flow from cell to cell and flow into storage. Cell dimensions, layer transmissivity and conductance between layers are specified in this package.
Output	OUT (included in BAS)	Input to control the amount and format of program output.
Well	WEL	Adds terms representing well flow to the finite-difference equations.
Recharge	RCH	Adds terms representing areally distributed recharge to the finite difference equations.
River	RIV	Adds terms representing flow to or from rivers or other surface water bodies to the finite difference equations.
Drain	DRN	Adds terms representing flow to drains to the finite-difference equations.
Evapotranspiration	EVT	Adds terms representing ET to the finite-difference equations.
General-Head Boundaries	GHB	Adds terms representing general head boundaries to the finite-difference equations.
Strongly Implicit Procedure	SIP	Iteratively solves the system of finite-difference equations using the Strongly Implicit Procedure.
Slice-Successive Overrelaxation	SOR	Iteratively solves the systems of finite-difference equations using slice-successive overrelaxation.

TABLE 3.1

COMPARISON OF REVISED VS ORIGINAL .BCF COLUMN SPACINGS				
Row No.	Revised .BCF		Original .BCF	
	DROW, cm.	Depth, cm.	DROW, cm.	Depth, cm.
1	1.0675	1.0675	1.0675	1.0675
2	4	5.0675	4	5.0675
3	4	9.0675	4	9.0675
4	3.9	12.9675	3.9	12.9675
5	3.5	16.4675	3.5	16.4675
6	3.5	19.9675	3.5	19.9675
7	3.1	23.0675	3.1	23.0675
8	3	26.0675	3	26.0675
9	2.6	28.6675	2.5	28.5675
10	2.3	30.9675	2.3	30.8675
11	2.1	33.0675	2.1	32.9675
12	1.75	34.8175	1.75	34.7175
13	1.6	36.4175	1.6	36.3175
14	1.35	37.7675	1.35	37.6675
15	1.1	38.8675	1.1	38.7675
16	0.8	39.6675	0.8	39.5675
17	0.6	40.2675	0.6	40.1675
18	0.3908	40.6583	0.3	40.4675
19	0.3	40.9583	0.3	40.7675
20	0.3	41.2583	0.3	41.0675
21	0.17	41.4283	0.17	41.2375
22	0.11	41.5383	0.11	41.3475
23	0.09	41.6283	0.11	41.4575
24	0.07	41.6983	0.08	41.5375
25	0.05	41.7483	0.08	41.6175
26	0.025	41.7733	0.07	41.6875
27	0.015	41.7883	0.05	41.7375
28	0.0008	41.7891	0.025	41.7625
29	0.0005	41.7896	0.025	41.7875
30	0.0003	41.7899	0.025	41.8125
31	0.0001	41.79	0.025	41.8375
32	0.0001	41.7901	0.025	41.8625
33	0.0003	41.7904	0.025	41.8875
34	0.0011	41.7915	0.025	41.9125
35	0.01	41.8015	0.025	41.9375
36	0.0289	41.8304	0.025	41.9625
37	0.0789	41.9093	0.025	41.9875
38	0.0789	41.9882	0.025	42.0125
39	0.0789	42.0671	0.025	42.0375
40	0.0289	42.096	0.025	42.0625
41	0.01	42.106	0.025	42.0875
42	0.0011	42.1071	0.025	42.1125
43	0.0003	42.1074	0.025	42.1375

TABLE 3.1

COMPARISON OF REVISED VS ORIGINAL .BCF COLUMN SPACINGS				
Row No.	Revised .BCF		Original .BCF	
	DROW, cm.	Depth, cm.	DROW, cm.	Depth, cm.
44	0.0001	42.1075	0.025	42.1625
45	0.0001	42.1076	0.025	42.1875
46	0.0003	42.1079	0.025	42.2125
47	0.0005	42.1084	0.025	42.2375
48	0.0008	42.1092	0.025	42.2625
49	0.015	42.1242	0.05	42.3125
50	0.025	42.1492	0.05	42.3625
51	0.05	42.1992	0.08	42.4425
52	0.07	42.2692	0.08	42.5225
53	0.09	42.3592	0.08	42.6025
54	0.11	42.4692	0.11	42.7125
55	0.11	42.5792	0.11	42.8225
56	0.25	42.8292	0.25	43.0725
57	0.25	43.0792	0.25	43.3225
58	0.35	43.4292	0.35	43.6725
59	0.6	44.0292	0.6	44.2725
60	0.7708	44.8	0.6	44.8725
61	1.25	46.05	1.25	46.1225
62	1.65	47.7	1.65	47.7725
63	2.1	49.8	2.1	49.8725
64	2.7	52.5	2.7	52.5725
65	3.7725	56.2725	3.7	56.2725
66	5.05	61.3225	5.05	61.3225
67	7.55	68.8725	7.55	68.8725
68	14.45	83.3225	14.45	83.3225
69	18.6775	102	18.6775	102

TABLE 3.2

COMPARISON OF REVISED VS ORIGINAL .BCF ROW SPACINGS				
	Revised .BCF		Original .BCF	
Column No.	DCOL, cm.	Distance, cm.	DCOL, cm.	Distance, cm.
1	0.3529	0.3529	0.3529	0.3529
2	0.3529	0.7058	0.3529	0.7058
3	0.3529	1.0587	0.3529	1.0587
4	0.3155	1.3742	0.3	1.3587
5	0.21	1.5842	0.21	1.5687
6	0.17	1.7542	0.17	1.7387
7	0.14	1.8942	0.14	1.8787
8	0.1	1.9942	0.1	1.9787
9	0.09	2.0842	0.09	2.0687
10	0.09	2.1742	0.09	2.1587
11	0.06	2.2342	0.06	2.2187
12	0.04	2.2742	0.04	2.2587
13	0.04	2.3142	0.04	2.2987
14	0.025	2.3392	0.025	2.3237
15	0.025	2.3642	0.025	2.3487
16	0.025	2.3892	0.025	2.3737
17	0.0175	2.4067	0.0175	2.3912
18	0.0175	2.4242	0.0175	2.4087
19	0.0175	2.4417	0.0175	2.4262
20	0.0175	2.4592	0.0175	2.4437
21	0.0175	2.4767	0.0175	2.4612
22	0.0175	2.4942	0.0175	2.4787
23	0.0175	2.5117	0.0175	2.4962
24	0.0175	2.5292	0.0175	2.5137
25	0.002	2.5312	0.0175	2.5312
26	0.002	2.5332	0.0029	2.5341
27	0.0029	2.5361	0.0029	2.537
28	0.0029	2.539	0.0029	2.5399
29	0.0029	2.5419	0.0029	2.5428
30	0.0029	2.5448	0.0029	2.5457
31	0.003	2.5478	0.003	2.5487
32	0.0044	2.5522	0.0044	2.5531
33	0.0044	2.5566	0.0044	2.5575
34	0.0087	2.5653	0.0087	2.5662
35	0.0087	2.574	0.0087	2.5749
36	0.0088	2.5828	0.0088	2.5837
37	0.0175	2.6003	0.0175	2.6012
38	0.0175	2.6178	0.0175	2.6187
39	0.0175	2.6353	0.0175	2.6362
40	0.0175	2.6528	0.0175	2.6537
41	0.0175	2.6703	0.0175	2.6712
42	0.0175	2.6878	0.0175	2.6887
43	0.0184	2.7062	0.0175	2.7062
44	0.025	2.7312	0.025	2.7312

TABLE 3.2

COMPARISON OF REVISED VS ORIGINAL .BCF ROW SPACINGS				
	Revised .BCF		Original .BCF	
Column No.	DCOL, cm.	Distance, cm.	DCOL, cm.	Distance, cm.
45	0.025	2.7562	0.025	2.7562
46	0.025	2.7812	0.025	2.7812
47	0.04	2.8212	0.04	2.8212
48	0.04	2.8612	0.04	2.8612
49	0.06	2.9212	0.06	2.9212
50	0.09	3.0112	0.09	3.0112
51	0.09	3.1012	0.09	3.1012
52	0.1	3.2012	0.1	3.2012
53	0.14	3.3412	0.14	3.3412
54	0.17	3.5112	0.17	3.5112
55	0.21	3.7212	0.21	3.7212
56	0.3	4.0212	0.3	4.0212
57	0.35	4.3712	0.35	4.3712
58	0.5	4.8712	0.5	4.8712
59	0.6574	5.5286	0.6574	5.5286
60	0.85	6.3786	0.85	6.3786
61	1	7.3786	1	7.3786
62	1.4	8.7786	1.4	8.7786
63	1.6426	10.4212	1.6426	10.4212
64	2.2	12.6212	2.2	12.6212
65	2.75	15.3712	2.75	15.3712
66	3.25	18.6212	3.25	18.6212
67	4.6	23.2212	4.6	23.2212
68	5.9	29.1212	5.9	29.1212
69	7.5	36.6212	7.5	36.6212
70	10	46.6212	10	46.6212
71	15.3	61.9212	15.3	61.9212
72	23.7	85.6212	23.7	85.6212
73	56.5	142.1212	56.5	142.1212
74	37.8788	180	37.8788	180

TABLE 3.3

			VERTICAL GRADIENT CALCULATIONS					
			COLUMN 62 HEADS FOR EACH LAYER					
	BOTTOM		APPROX 9 CM FROM SOURCE PIPE CENTER					
ROW	DEPTH	========						
NO.	CM	SLICE 1	h1-h2	delta z	J			J*3.89
1	1.0675	0						
2	5.0675	0.48	-0.48	2.53375	0.189443			0.73705
3	9.0675	1.24	-0.76	4	0.19			0.739219
4	12.9675	2.01	-0.77	3.95	0.194937	SUM OF 15 J'S		0.758426
5	16.4675	2.76	-0.75	3.7	0.202703	ABOVE PIPE		0.788641
6	19.9675	3.5	-0.74	3.5	0.211429			0.82259
7	23.0675	4.25	-0.75	3.3	0.227273			0.884233
8	26.0675	4.99	-0.74	3.05	0.242623			0.943955
9	28.6675	5.71	-0.72	2.8	0.257143			1.000447
10	30.9675	6.4	-0.69	2.45	0.281633			1.095728
11	33.0675	7.06	-0.66	2.2	0.3			1.167188
12	34.8175	7.68	-0.62	1.925	0.322078			1.253085
13	36.4175	8.24	-0.56	1.675	0.334328			1.300747
14	37.7675	8.74	-0.5	1.475	0.338983			1.318857
15	38.8675	9.15	-0.41	1.225	0.334694	3.93253	0.262169	1.286082
16	39.6675	9.44	-0.29	0.95	0.305263			1.187665
17	40.2675	9.63	-0.19	0.7	0.271429	divided by 15=		1.056027
18	40.6583	9.74	-0.11	0.4954	0.222043			0.863886
19	40.9583	9.81	-0.07	0.3454	0.202664			0.788488
20	41.2583	9.86	-0.05	0.3	0.166667		3.890625	0.648438
21	41.4283	9.89	-0.03	0.235	0.12766			0.496676
22	41.5383	9.9	-0.01	0.14	0.071429			0.277902
23	41.6283	9.91	-0.01	0.1	0.1	1.02/0.262169=		0.389063
24	41.6983	9.92	-0.01	0.08	0.125	(FACTOR TO MAKE		0.486328
25	41.7483	9.92	0	0.06	0	J ADEQUATE FOR		0
26	41.7733	9.92	0	0.0375	0	FLUIDIZATION		0
27	41.7883	9.93	-0.01	0.02	0.5			1.945314
28	41.7891	9.93	0	0.0079	0			0
29	41.7896	9.93	0	0.00065	0			0
30	41.7899	9.93	0	0.0004	0			0
31	41.79	9.93	0	0.0002	0			0
32	41.7901	9.93	0	0.0001	0			0
33	41.7904	9.93	0	0.0002	0			0
34	41.7915	9.93	0	0.0007	0			0
35	41.8015	9.93	0	0.00555	0			0
36	41.8304	9.93	0	0.01945	0			0
37	41.9093	9.93	0	0.0539	0			0
38	41.9882	9.94	-0.01	0.0789	0.126743			0.493109
39	42.0671	9.94	0	0.0789	0			0
40	42.096	9.94	0	0.0539	0			0
41	42.106	9.95	-0.01	0.01945	0.514139			2.000322
42	42.1071	9.95	0	0.00555	0			0
43	42.1074	9.95	0	0.0007	0			0

TABLE 3.3

		VERTICAL GRADIENT CALCULATIONS					
		COLUMN 62 HEADS FOR EACH LAYER					
	BOTTOM	APPROX 9 CM FROM SOURCE PIPE CENTER					
ROW	DEPTH	========					
NO.	CM	SUCE 1	h1-h2	delta z	J		J*3.89
44	42.1075	9.95	0	0.0002	0		0
45	42.1076	9.95	0	0.0001	0		0
46	42.1079	9.95	0	0.0002	0		0
47	42.1084	9.95	0	0.0004	0		0
48	42.1092	9.95	0	0.00085	0		0
49	42.1242	9.95	0	0.0079	0		0
50	42.1492	9.95	0	0.02	0		0
51	42.1992	9.95	0	0.0375	0		0
52	42.2692	9.95	0	0.06	0		0
53	42.3592	9.95	0	0.08	0		0
54	42.4592	9.96	-0.01	0.1	0.1		0.389063
55	42.5792	9.96	0	0.11	0		0
56	42.8292	9.96	0	0.18	0		0
57	43.0792	9.95	0.01	0.25	-0.04		-0.15563
58	43.4292	9.94	0.01	0.3	-0.03333		-0.12969
59	44.0292	9.9	0.04	0.475	-0.08421		-0.32763
60	44.8	9.82	0.08	0.6854	-0.11672		-0.45411
61	46.05	9.65	0.17	1.0104	-0.16825		-0.6546
62	47.7	9.35	0.3	1.45	-0.2069		-0.80496
63	49.8	8.94	0.41	1.875	-0.21867		-0.85075
64	52.5	8.44	0.5	2.4	-0.20833		-0.81056
65	56.2725	7.84	0.6	3.23625	-0.1854		-0.72132
66	61.3225	7.18	0.66	4.41125	-0.14962		-0.58211
67	68.6725	6.47	0.71	6.3	-0.1127		-0.43847
68	83.3225	5.65	0.82	11	-0.07455		-0.29003
69	102	5.1	0.55	16.56375	-0.03321		-0.12919

TABLE 3.4

	VERTICAL GRADIENTS AT KEY LOCATIONS					
Y, cm. (relative to pipe center)	J@x=2.54 cm. Slice 1	Slice 3	Slice 4	Slice 7	J @ x=9cm (all slices are equal)	J@x=0cm
40.146125	0.75228416	0.75228416	0.75228416	0.75228416	0.73705	0.75228416
36.88125	0.766275	0.766275	0.766275	0.766275	0.739219	0.766275
32.90625	0.7878481	0.7878481	0.7878481	0.7878481	0.758425	0.7878481
29.08125	0.82005405	0.82005405	0.82005405	0.82005405	0.788641	0.83056757
25.48125	0.87802857	0.87802857	0.87802857	0.87802857	0.82259	0.87802857
22.08125	0.9430303	0.9430303	0.9430303	0.9430303	0.884233	0.95481818
18.90625	1.03308197	1.03308197	1.03308197	1.03308197	0.943955	1.04583607
15.98125	1.15310714	1.15310714	1.15310714	1.15310714	1.000447	1.18089286
13.35625	13.35625	1.28608163	1.28608163	13.3207	1.30195918	1.28608163
11.03125	1.44990909	1.44990909	1.44990909	1.45759091	1.167188	1.48527273
8.96875	1.67724675	1.67724675	1.67724675	1.65703896	1.253085	1.69745455
7.16875	1.88113433	1.88113433	1.88113433	1.88113433	1.300747	1.88113433
5.59375	2.21532203	2.21532203	2.21532203	1.95159322	1.318857	1.9779661
4.24375	2.54040816	2.54040816	2.54040816	2.85795918	1.302169	1.90530612
3.15625	4.09473684	4.09473684	4.09473684	3.27578947	1.187665	0.81894737
2.33125	7.22428571	7.22428571	7.22428571	4.44571429	1.056027	5490.45714
1.73355	11.7783609	11.7783609	11.7783609	4.71134437	0.863866	0
1.31315	22.5246091	21.3983787	21.3983787	5.63115229	0.788488	0
0.99045	38.9	37.6033333	36.3066667	6.48333333	0.648438	0
0.72295	79.4553191	72.8340425	71.1767234	4.96595745	0.496676	0
0.53545	144.485714	127.814286	119.478571	5.55714286	0.277902	0
0.41545	221.73	186.72	167.27	3.89	0.389063	0
0.32545	447.35	335.5125	291.75	4.8625	0.486328	0
0.25545	609.433333	427.9	330.65	0	0	0
0.2067	1400.4	892.106667	518.666667	10.3733333	0	0
0.17795	181157.3	183510.75	184372.25	191388	1.945314	0
0.164	0	0	0	0	0	0
0.159725	0	0	0	0	0	0
0.1592	0	0	0	0	0	0
0.1589	0	0	0	0	0	0
0.15875	-34971100	0	0	0	0	0
0.1586	0	0	0	0	0	0
0.15815	0	0	0	0	0	0
0.155025	0	0	0	0	0	0
0.142525	0	0	0	0	0	0
0.10525	0	0	0	0	0	0
0.03945	0	0	0	0	0.493109	0
-0.03945	0	0	0	0	0	0
-0.10585	0	0	0	0	0	0
-0.142525	0	0	0	0	2.000322	0
-0.155025	0	0	0	0	0	0
-0.15815	0	0	0	0	0	0
-0.1586	0	0	0	0	0	0

TABLE 3.4

		VERTICAL GRADIENTS AT KEY LOCATIONS				
Y, cm.	==========	J@x=2.54 cm.		==========	J @ x=9cm	J@x=0cm
[relative to						
pipe center]	Slice 1	Slice 3	Slice 4	Slice 7	[all slices are equal]	
-0.15875	34971100	0	0	0	0	0
-0.1589	0	0	0	0	0	0
-0.1592	0	0	0	0	0	0
-0.159725	0	0	0	0	0	0
-0.164	0	0	0	0	0	0
-0.17795	-180982.25	-183394.05	-184775	-191388	0	0
-0.2067	-1255.1733	-798.74667	-466.8	0	0	0
-0.25545	-810.41667	-557.56667	-421.41667	-6.4833333	0	0
-0.32545	-389	-296.6125	-257.7125	0	0	0
-0.41545	-233.4	-194.5	-175.05	-3.89	0.389063	0
-0.52045	-152.06364	-130.84545	-123.77273	-3.5363636	0	0
-0.66545	-95.088889	-88.605556	-86.444444	-4.3222222	0	0
-0.88045	-48.236	-46.68	-43.568	-4.668	-0.15563	0
-1.15545	-27.23	-25.933333	-25.933333	-5.1866667	-0.12969	0
-1.54295	-15.56	-14.741053	-14.741053	-5.7326316	-0.32763	0
-2.12315	-7.3781733	-7.3781733	-7.3781733	-3.9728626	-0.45411	-5603.4389
-2.97105	-4.2349565	-4.2349565	-4.2349565	-3.0799683	-0.6546	-0.7699921
-4.20125	-2.4144828	-2.4144828	-2.4144828	-2.1462069	-0.80496	-1.6096552
-5.86375	-1.6597333	-1.6597333	-1.6597333	-1.6597333	-0.85075	-1.6597333
-8.00125	-1.2804583	-1.2804583	-1.2804583	-1.2804583	-0.81055	-1.2966667
-10.819375	-1.0337273	-1.0337273	-1.0337273	-1.0337273	-0.72132	-1.0697876
-14.643125	-0.7583791	-0.7583791	-0.7583791	-0.7583791	-0.58211	-0.7760159
-19.99875	-0.5248413	-0.5248413	-0.5248413	-0.5248413	-0.43847	-0.5310159
-28.64875	-0.3218091	-0.3218091	-0.3218091	-0.3218091	-0.29003	-0.3288818
-42.430625	-0.1409101	-0.1409101	-0.1409101	-0.1409101	-0.12919	-0.1409101

FIGURES

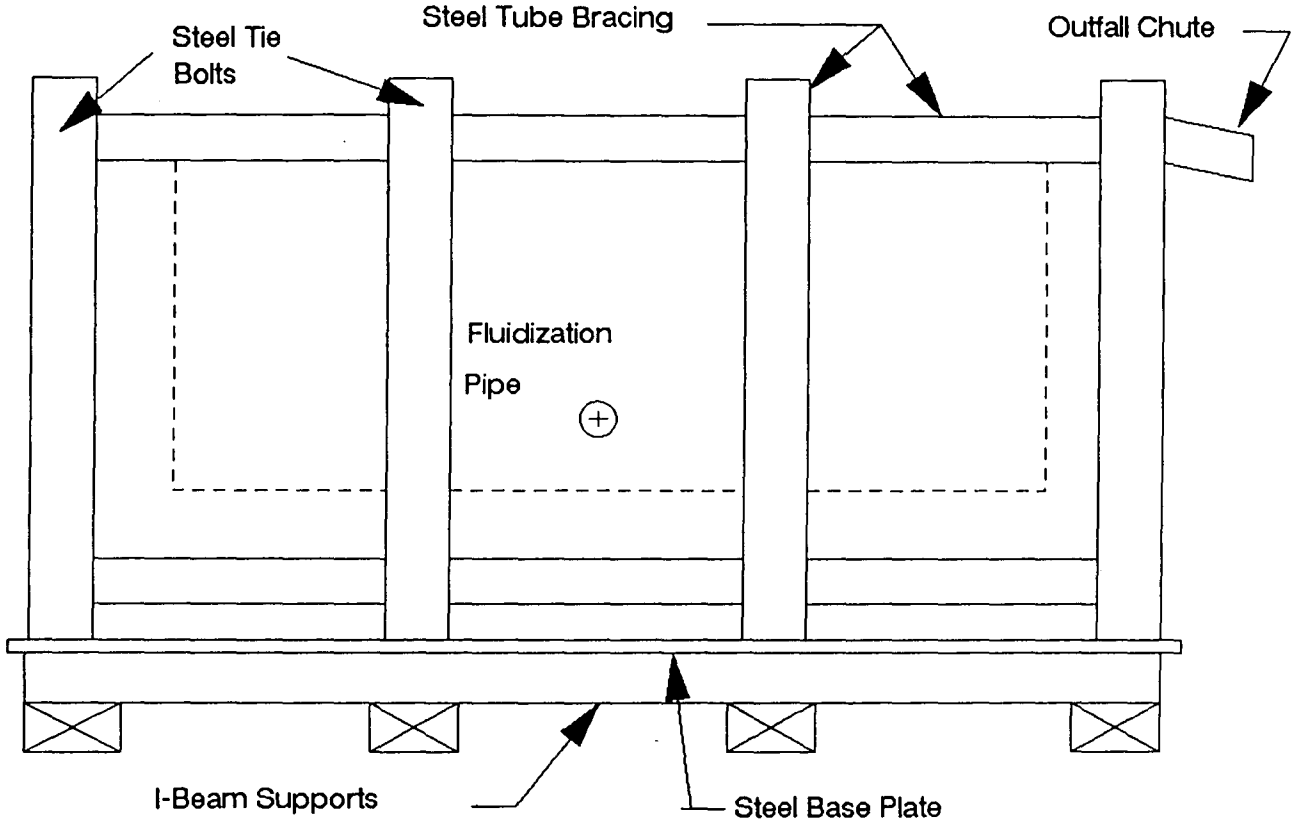

Figure 1.1 - Sketch of Two-Dimensional Fluidization Tank
Figure from Clifford (1989)

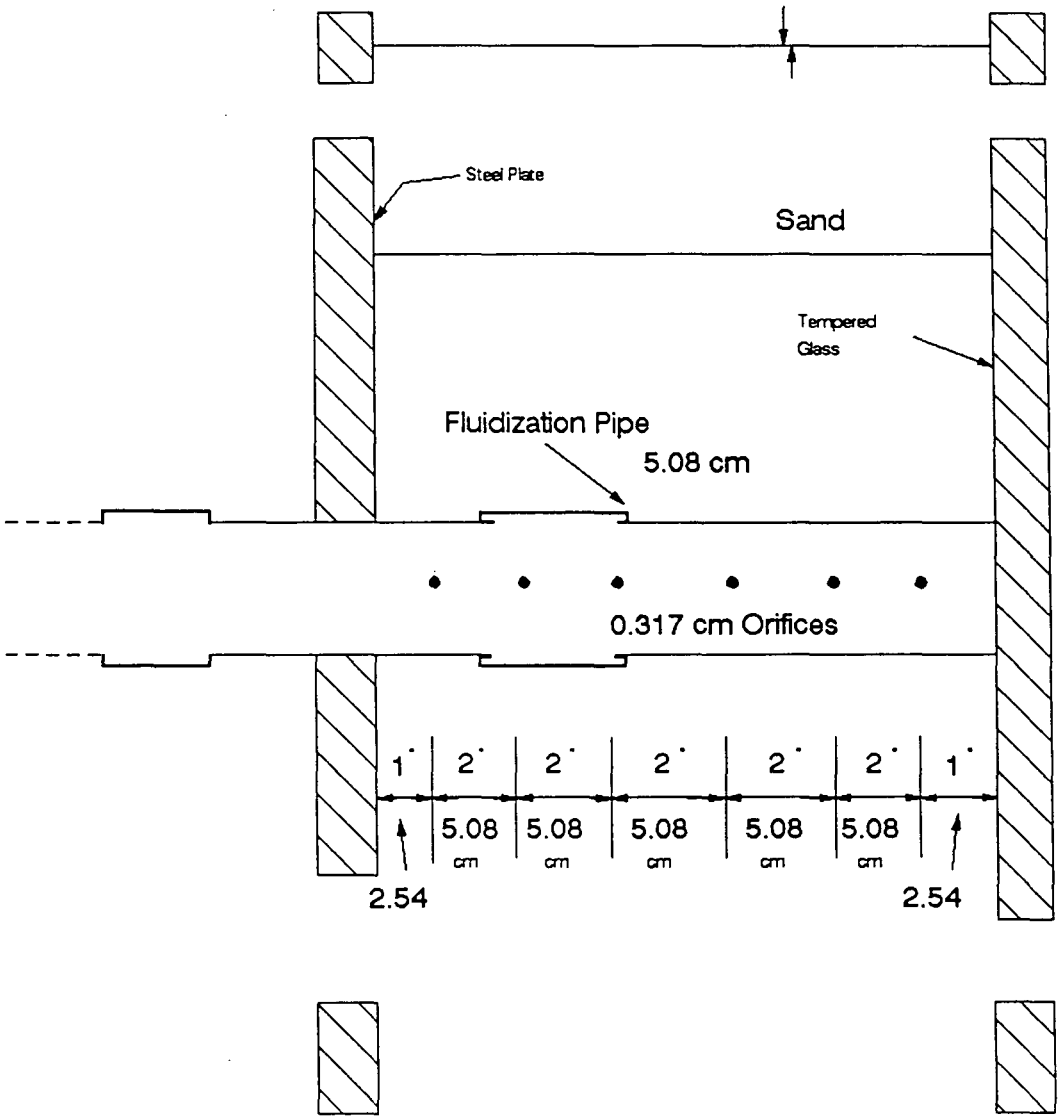

Figure 1.2 - Fluidization Pipe Details.
Figure from Clifford (1989)

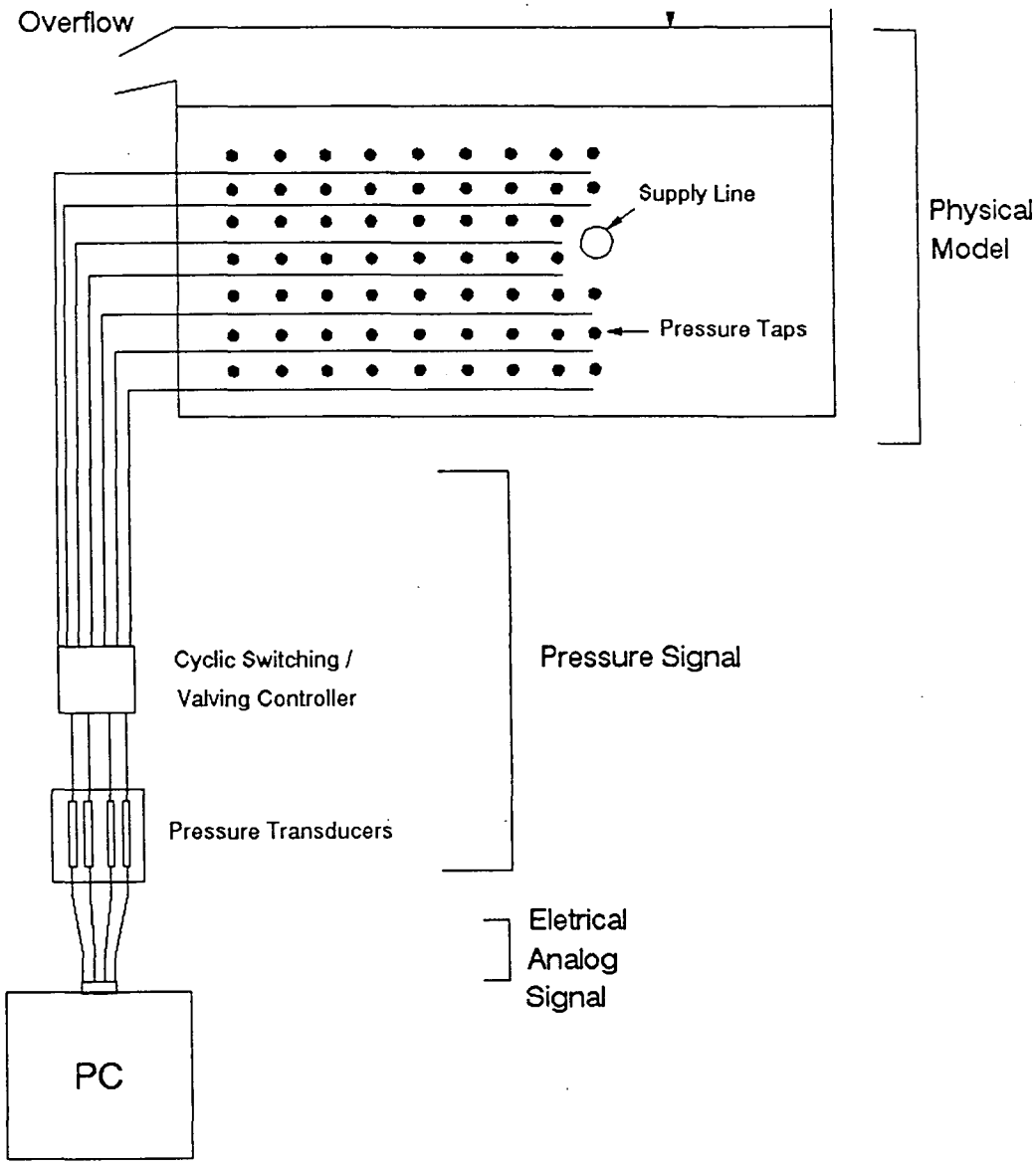

Figure 1.3 - Schematic of Data Acquisition System

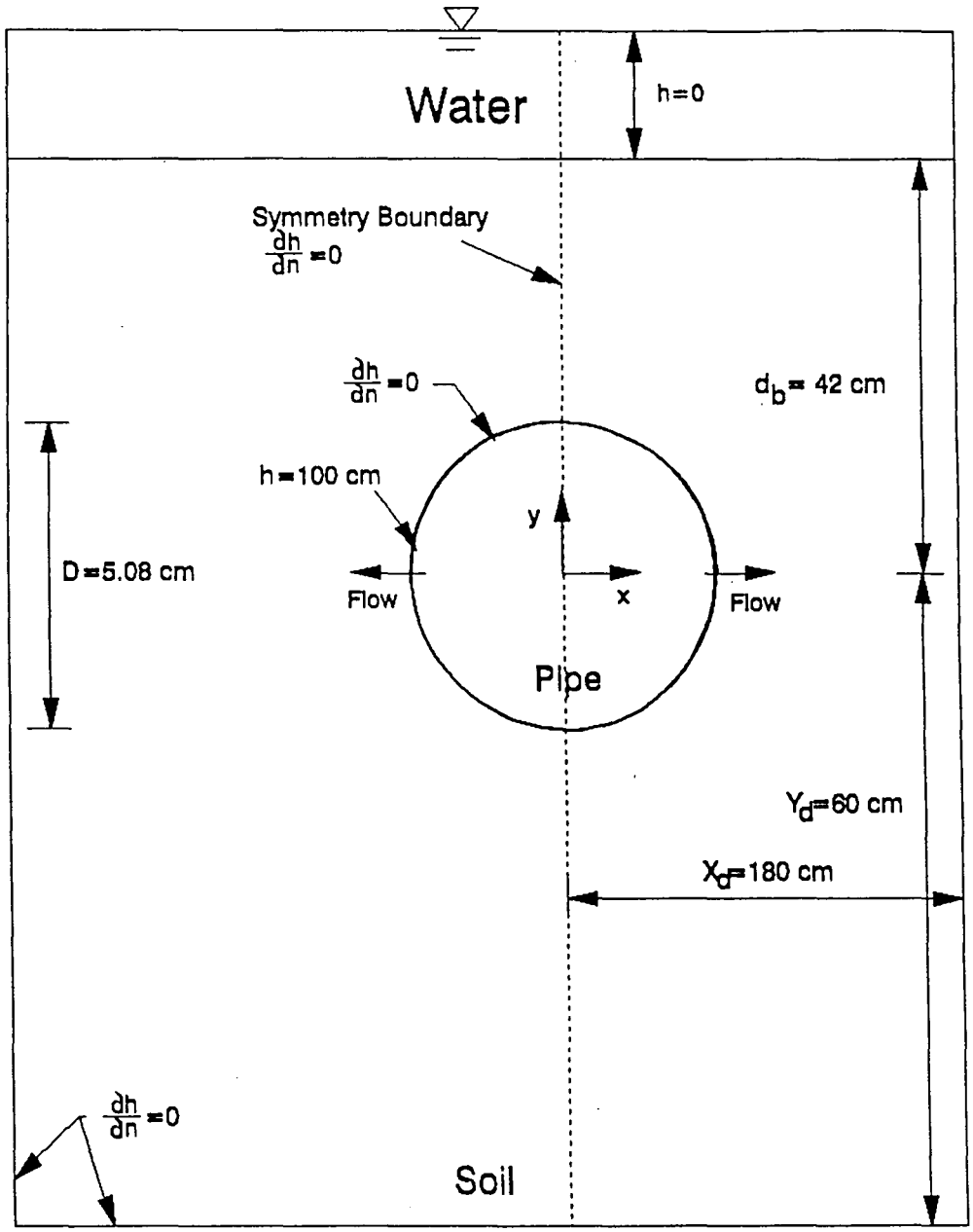

Sketch of Experimental Tank Dimensions and Boundary Conditions

Figure 2.1

Fluidization Model - Top View

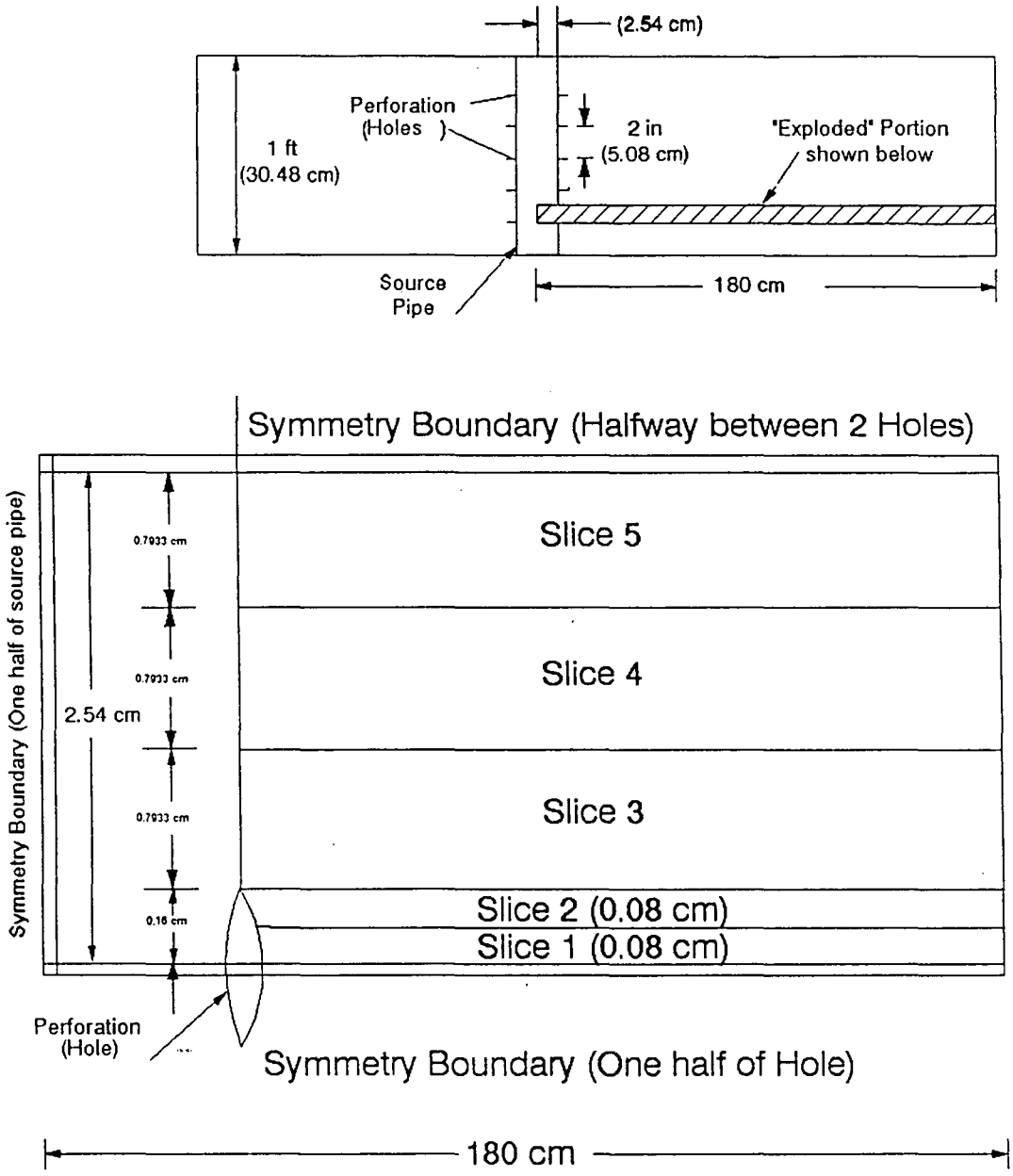

Exploded View

Slices 1 thru 5 are MOD Model layers. Not to scale.

Figure 2.2

FIGURE 3.1

FINITE DIFFERENCE GRID - SIDE VIEW

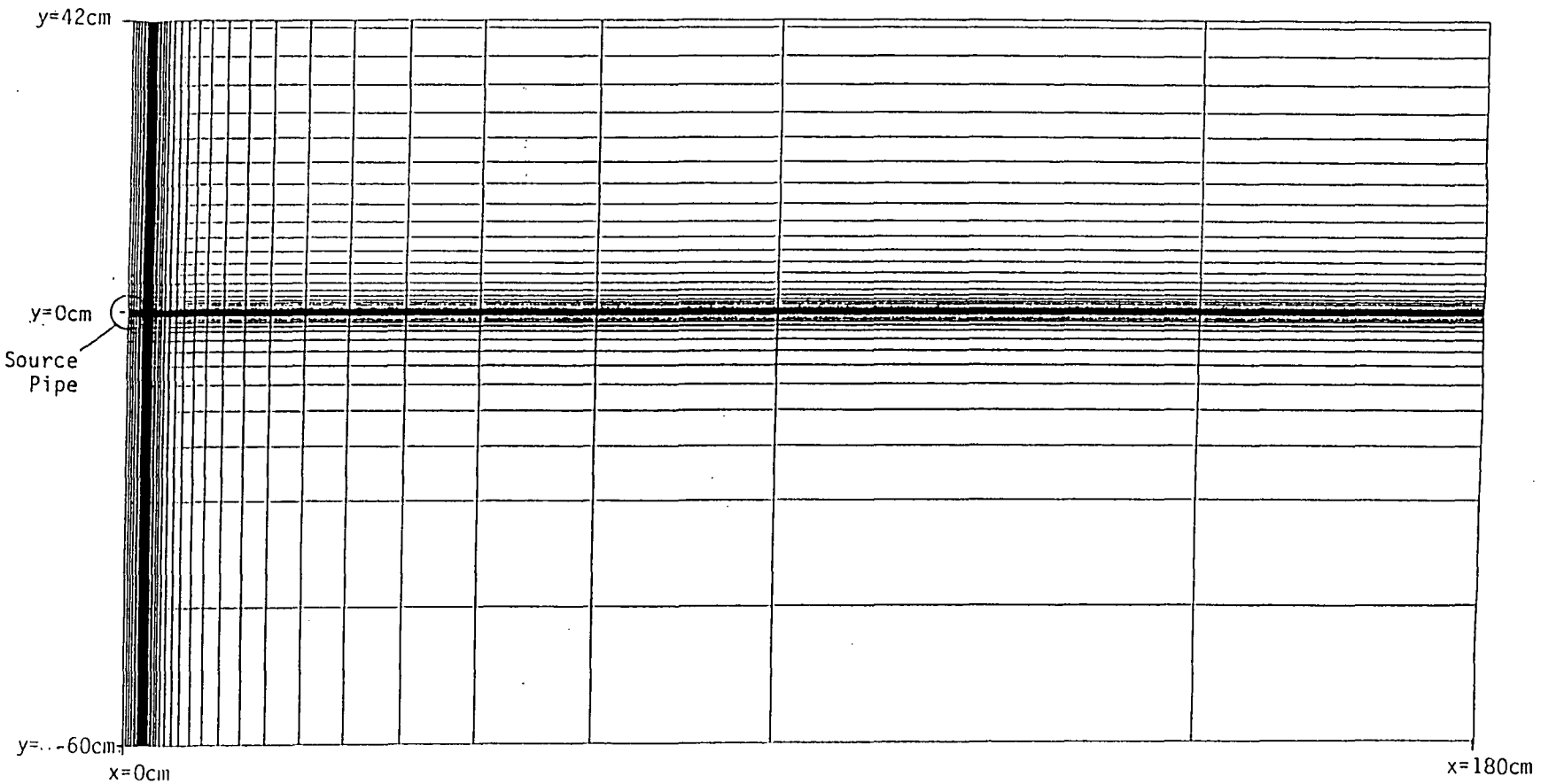

FIGURE 3.2

FINITE DIFFERENCE GRID - SIDE VIEW

ENGLARGED NEAR SOURCE ORIFICE

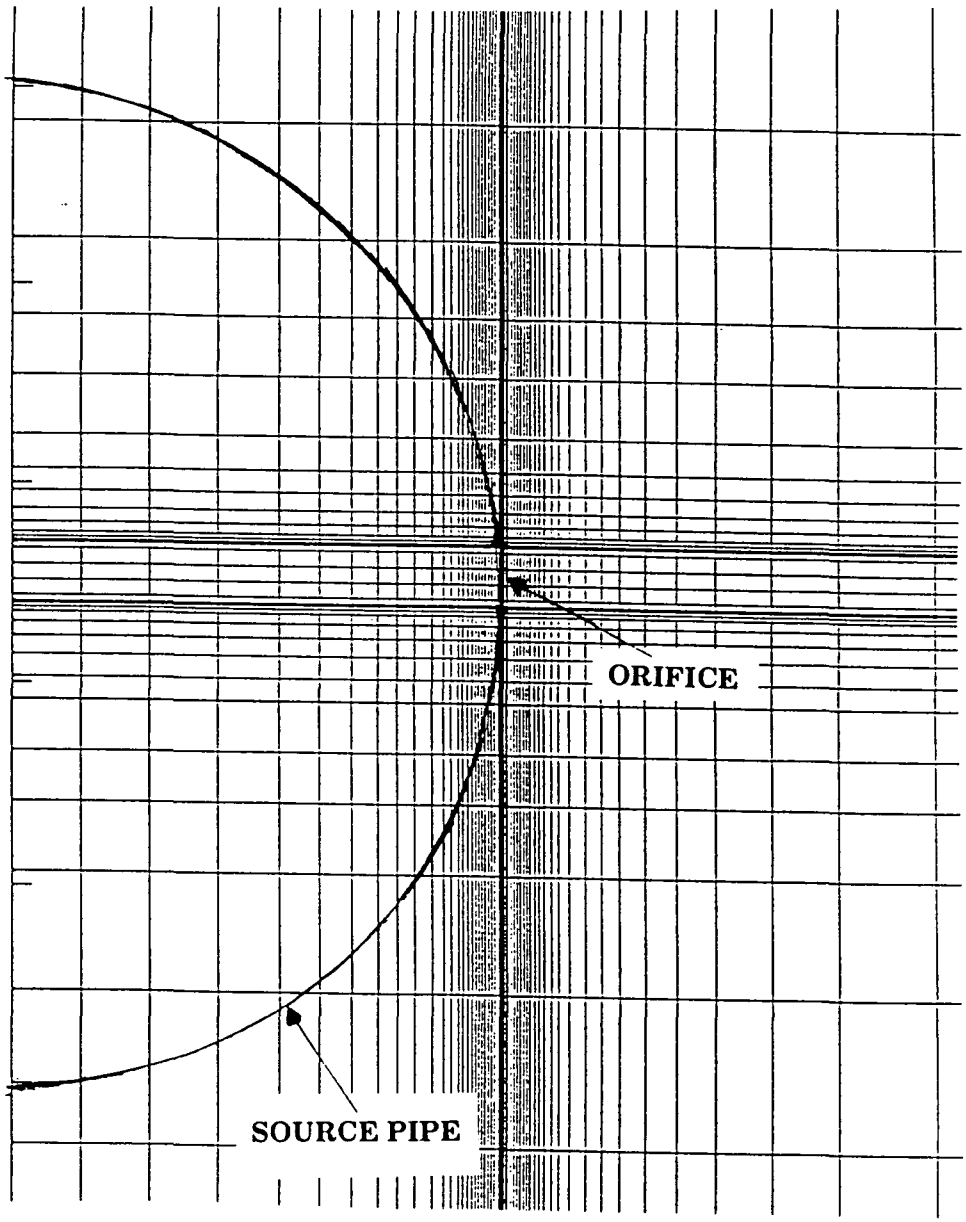

FIGURE 3.3
FINITE DIFFERENCE GRID - SIDE VIEW
FURTHER ENLARGED AT SOURCE ORIFICE

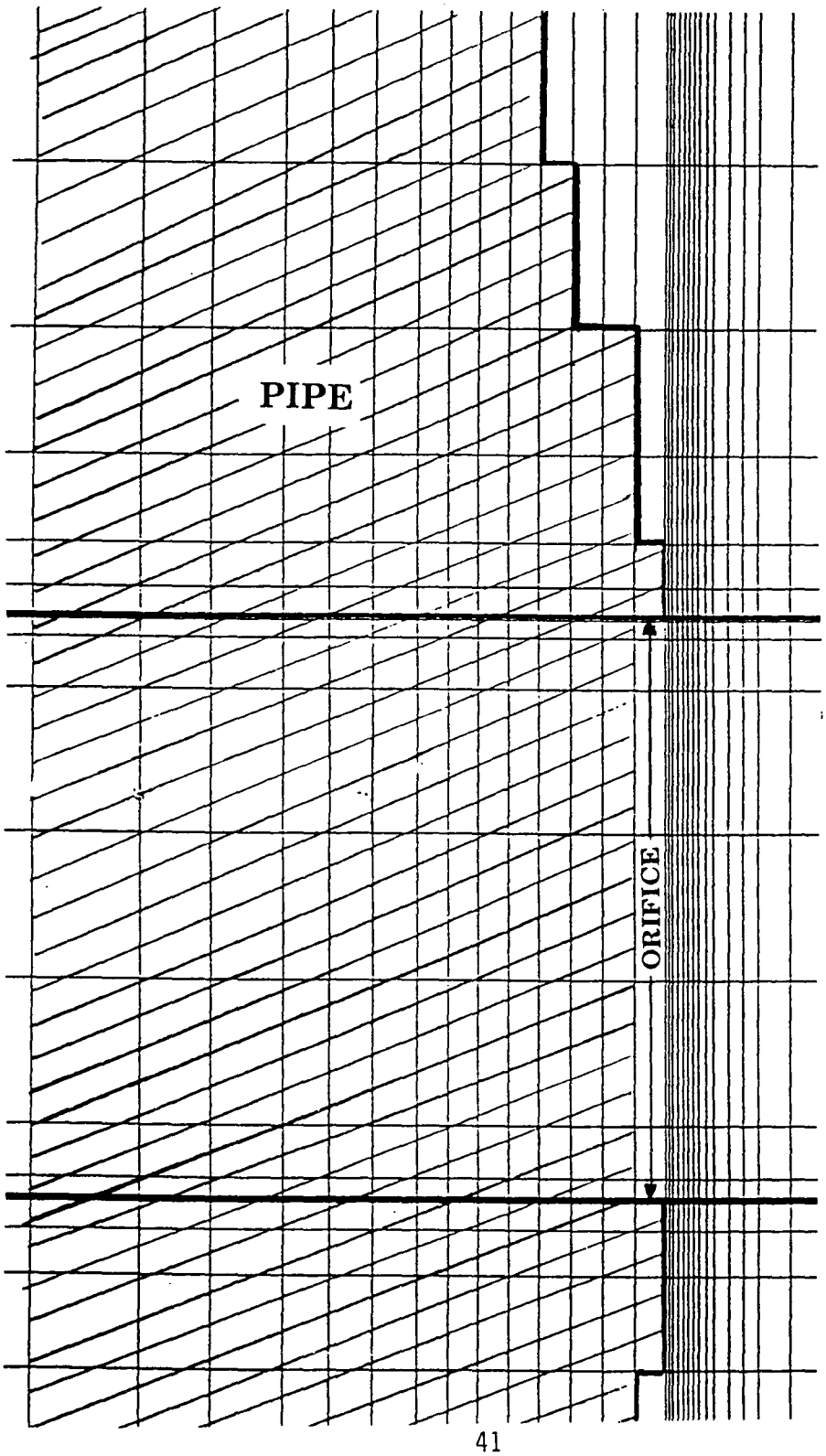

Model Run Slice Resolution

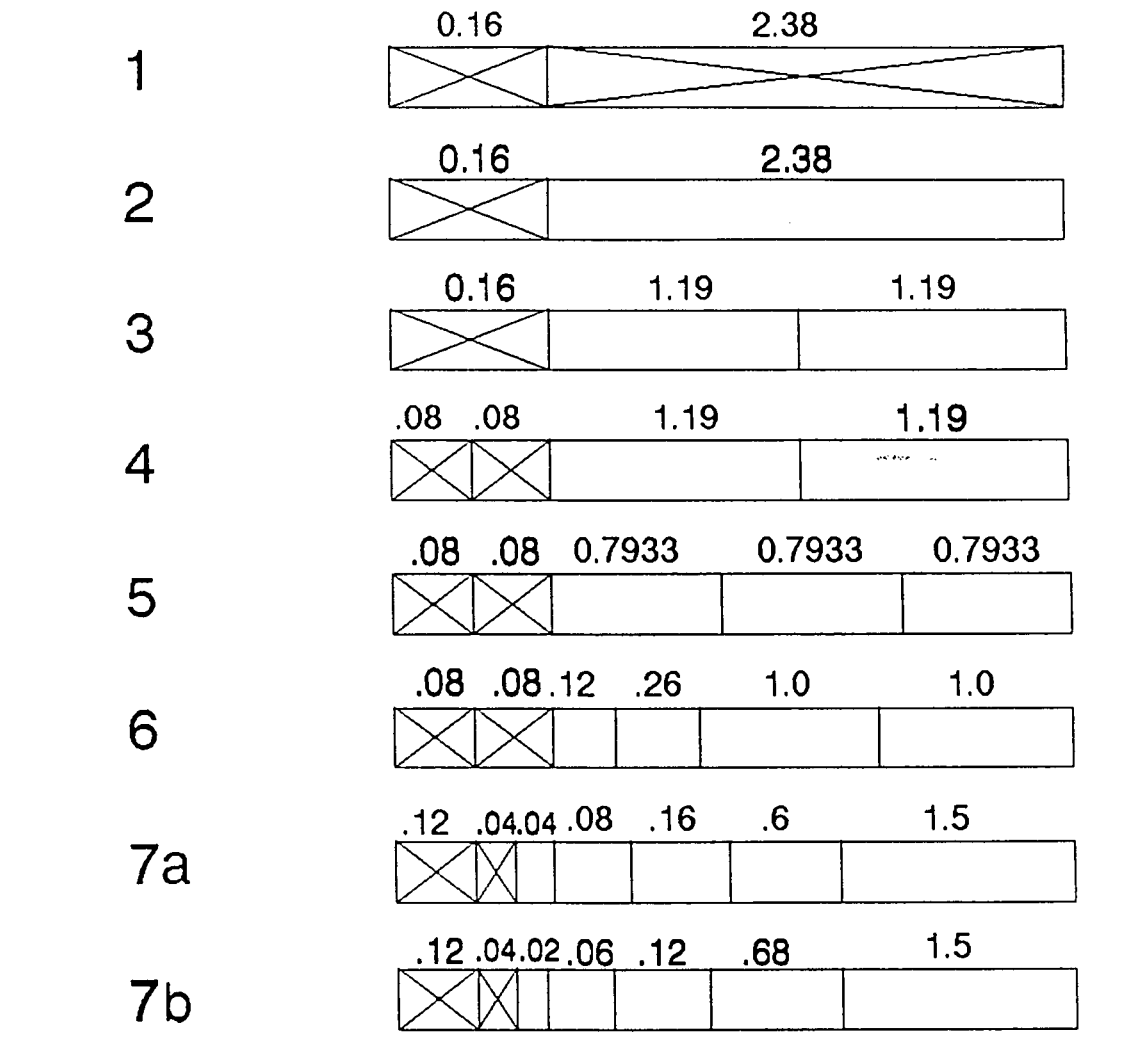

Figure 3.4

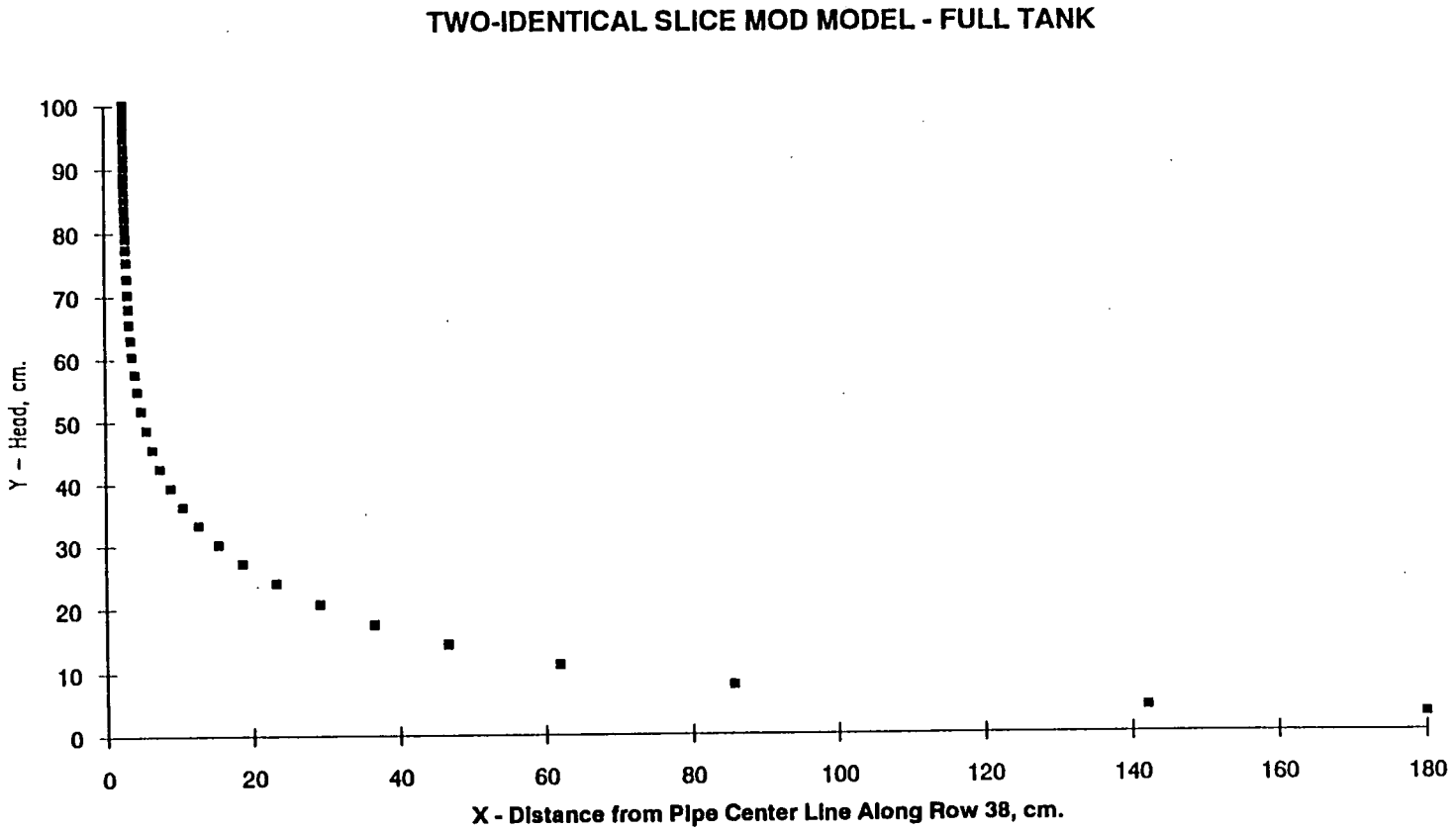
TWO-IDENTICAL SLICE MOD MODEL - FULL TANK
Y - Head, cm.
100
90
80
70
60
50
40
30
20
10
0
0
20
40
60
80
100
120
140
160
180
X - Distance from Pipe Center Line Along Row 38, cm.

FIGURE 3.5

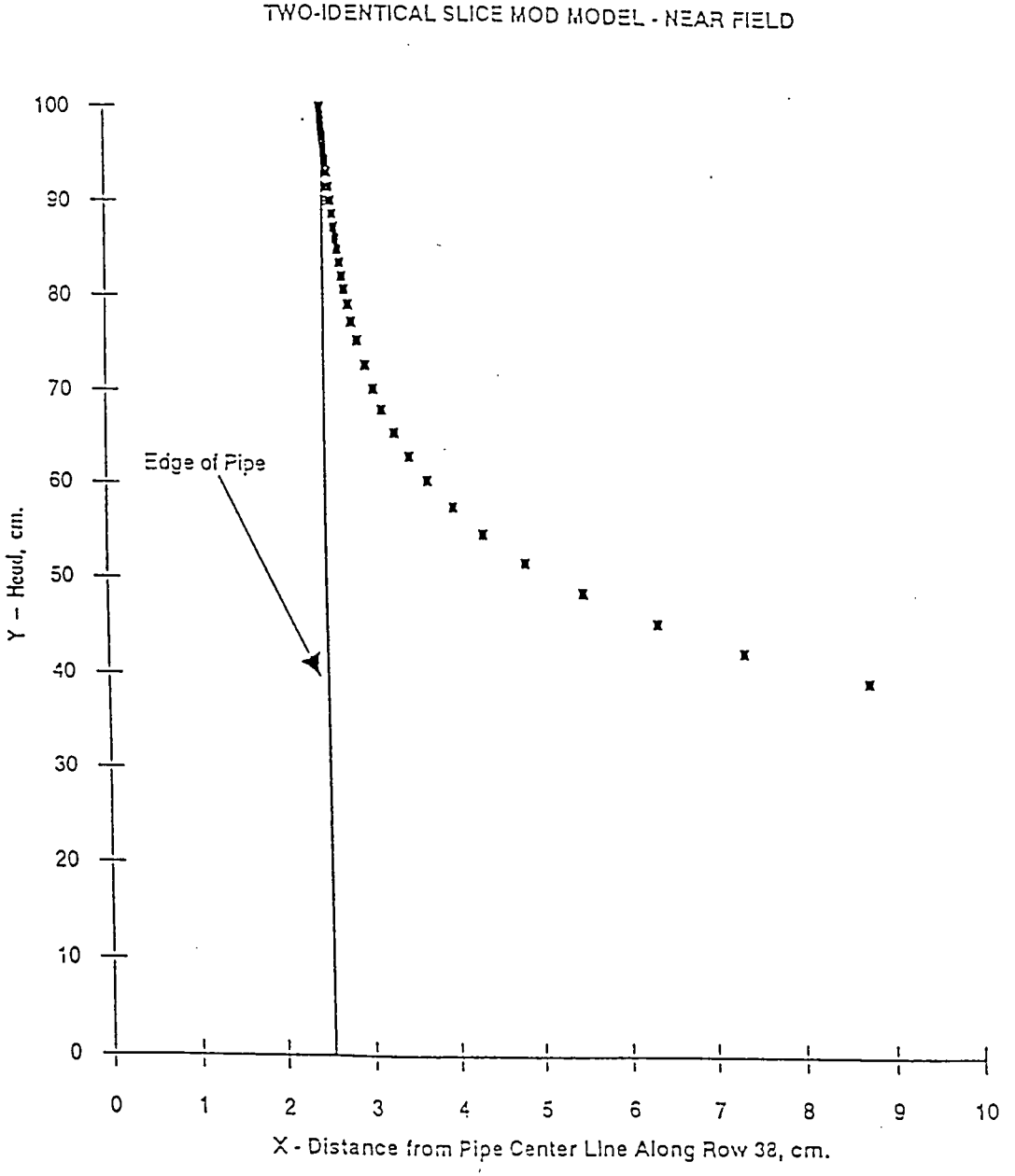
TWO-IDENTICAL SLICE MOD MODEL - NEAR FIELD
Edge of Pipe
Y – Head, cm.
100
90
80
70
60
50
40
30
20
10
0
0
1
2
3
4
5
6
7
8
9
10
X - Distance from Pipe Center Line Along Row 38, cm.

FIGURE 3.6

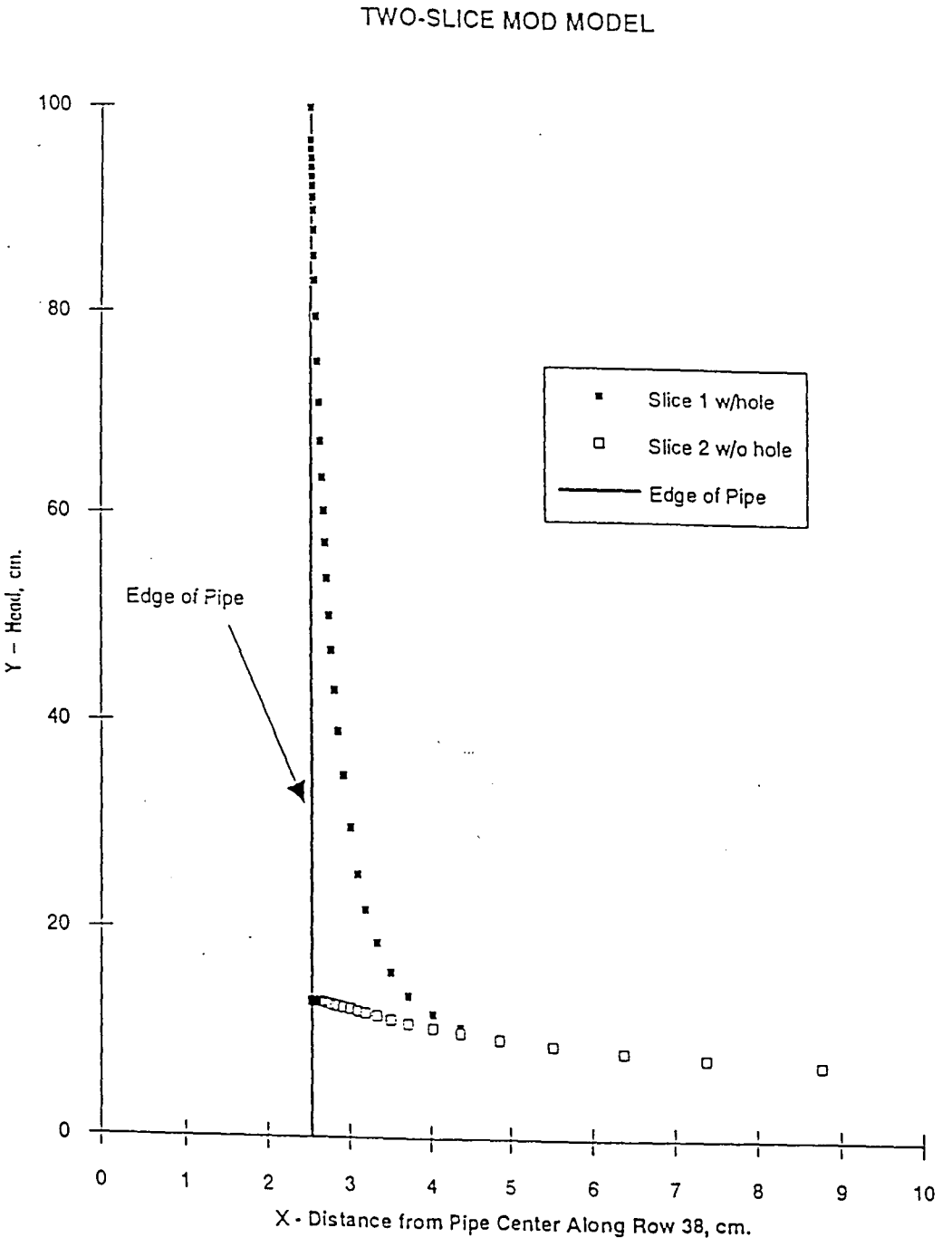
TWO-SLICE MOD MODEL
100
80
60
40
20
0
Y – Head, cm.
Edge of Pipe
Slice 1 w/hole
Slice 2 w/o hole
Edge of Pipe
0
1
2
3
4
5
6
7
8
9
10
X - Distance from Pipe Center Along Row 38, cm.

FIGURE 3.7

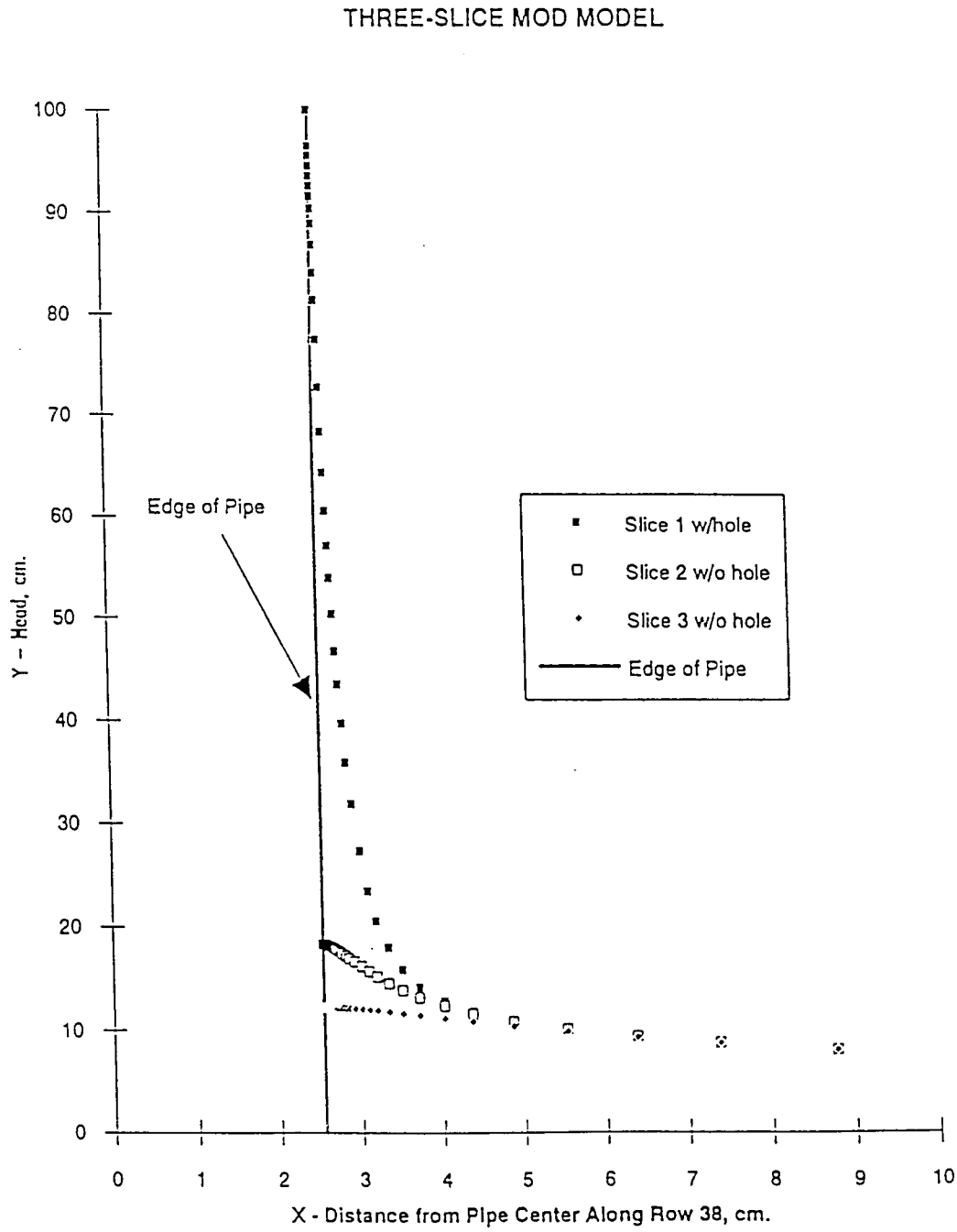
THREE-SLICE MOD MODEL
Y - Head, cm.
X - Distance from Pipe Center Along Row 38, cm.
Edge of Pipe
Slice 1 w/hole
Slice 2 w/o hole
Slice 3 w/o hole
Edge of Pipe
0
10
20
30
40
50
60
70
80
90
100
0
1
2
3
4
5
6
7
8
9
10

FIGURE 3.8

LAY4MOR1.XLS Chart 1

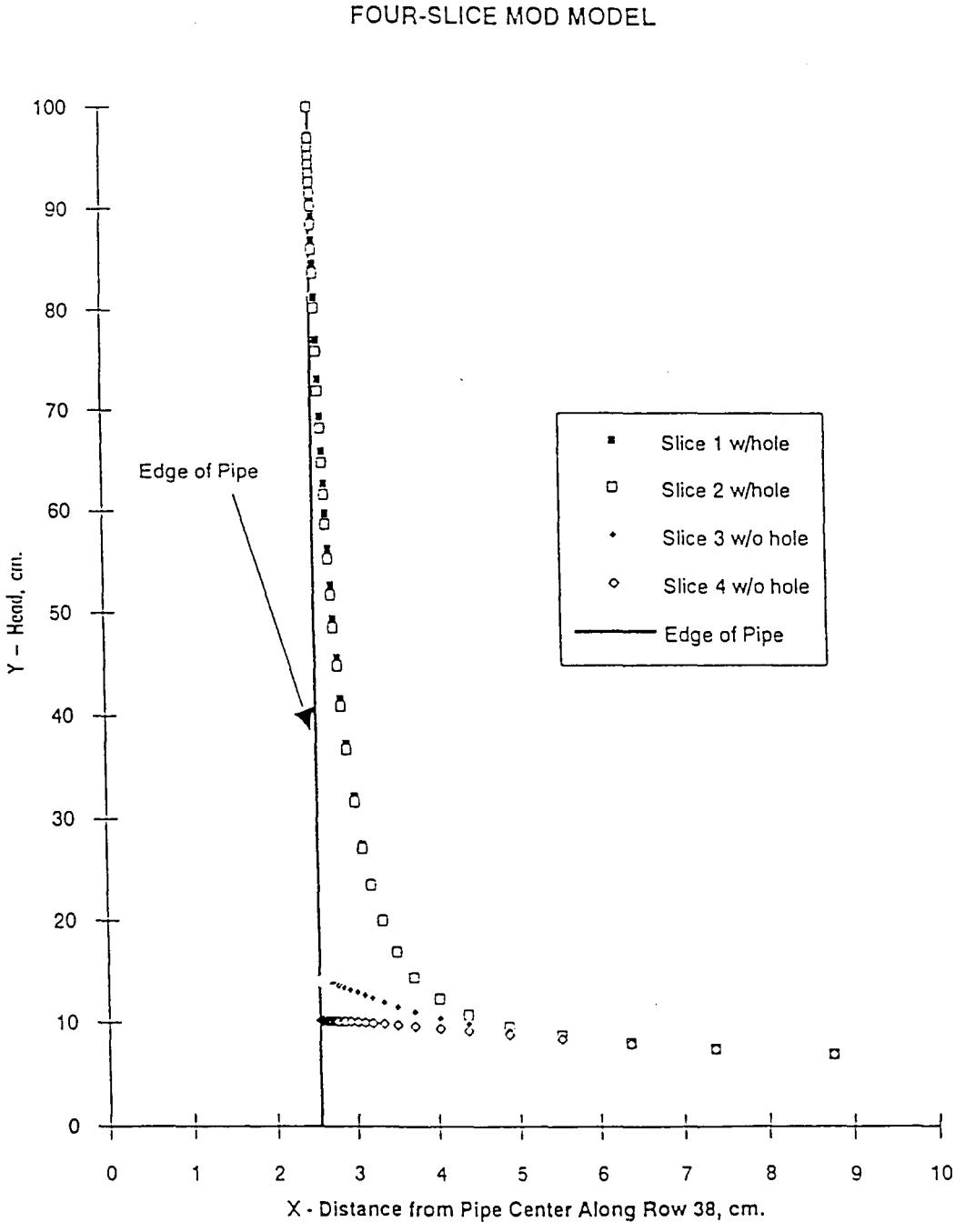

FIGURE 3.9

LAY5MOR2.XLS Chart 1

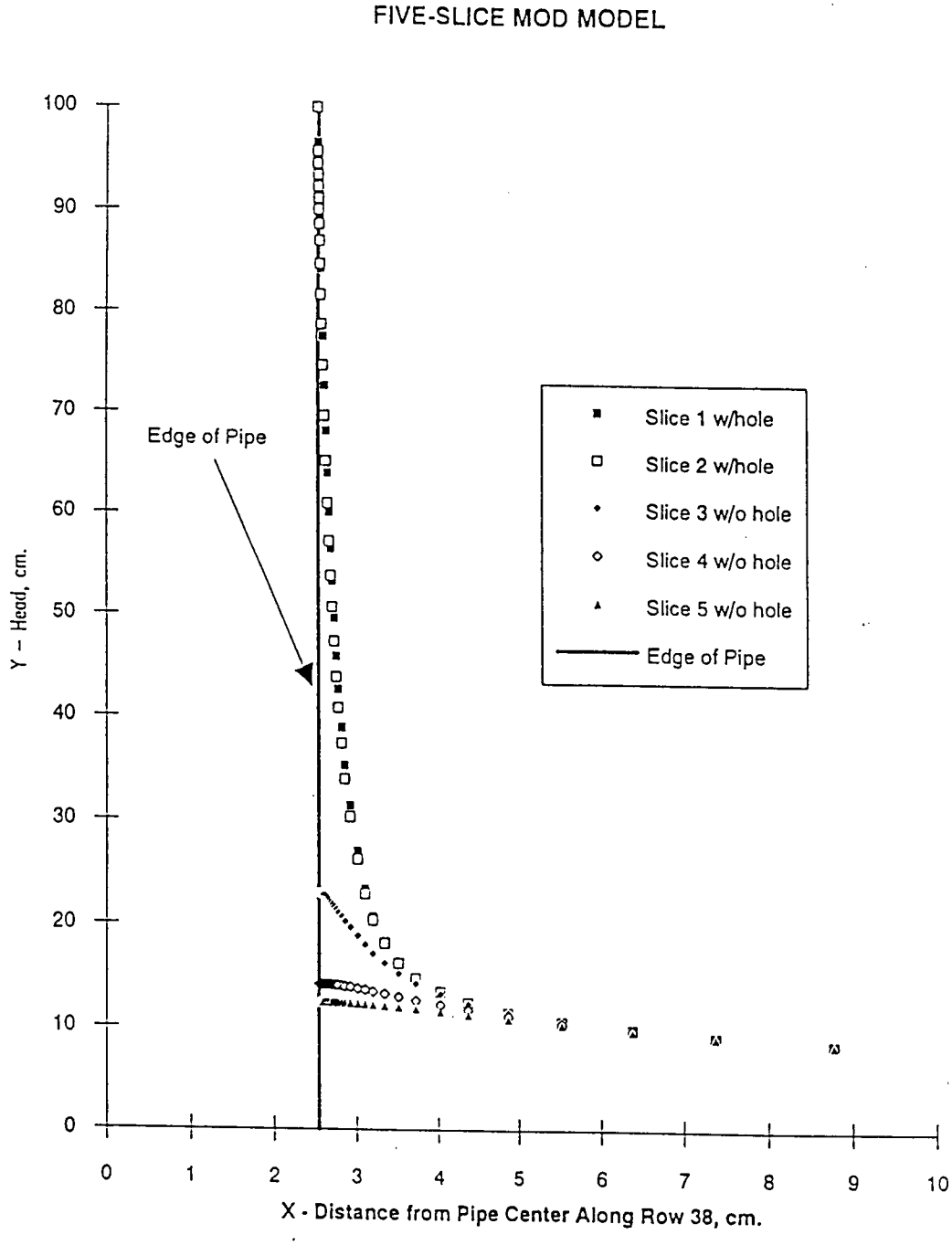

FIGURE 3.10

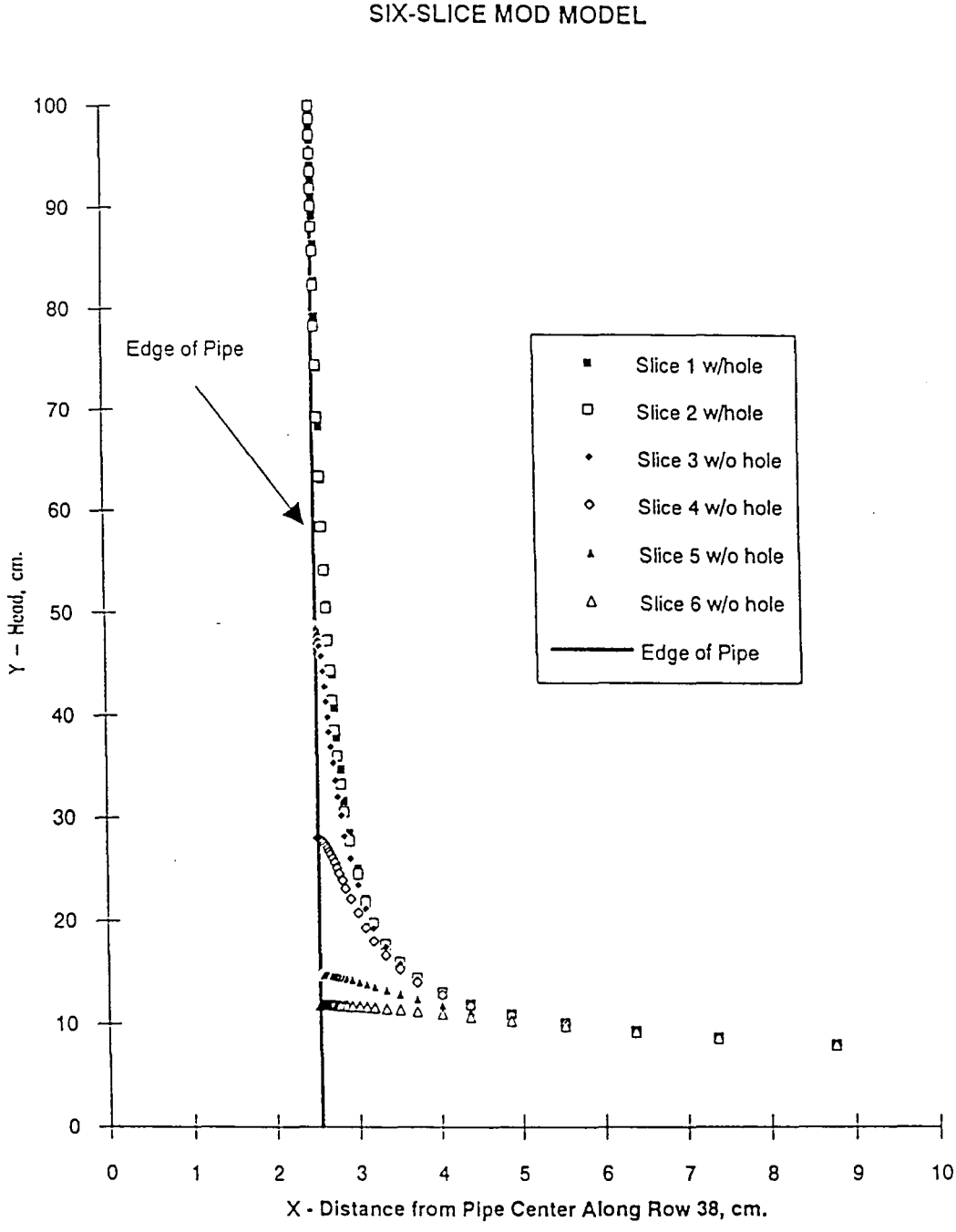
SIX-SLICE MOD MODEL
Edge of Pipe
Slice 1 w/hole
Slice 2 w/hole
Slice 3 w/o hole
Slice 4 w/o hole
Slice 5 w/o hole
Slice 6 w/o hole
Edge of Pipe
Y - Head, cm.
X - Distance from Pipe Center Along Row 38, cm.
0
10
20
30
40
50
60
70
80
90
100
0
1
2
3
4
5
6
7
8
9
10

FIGURE 3.11

LA6CROW.XLS Chart 1

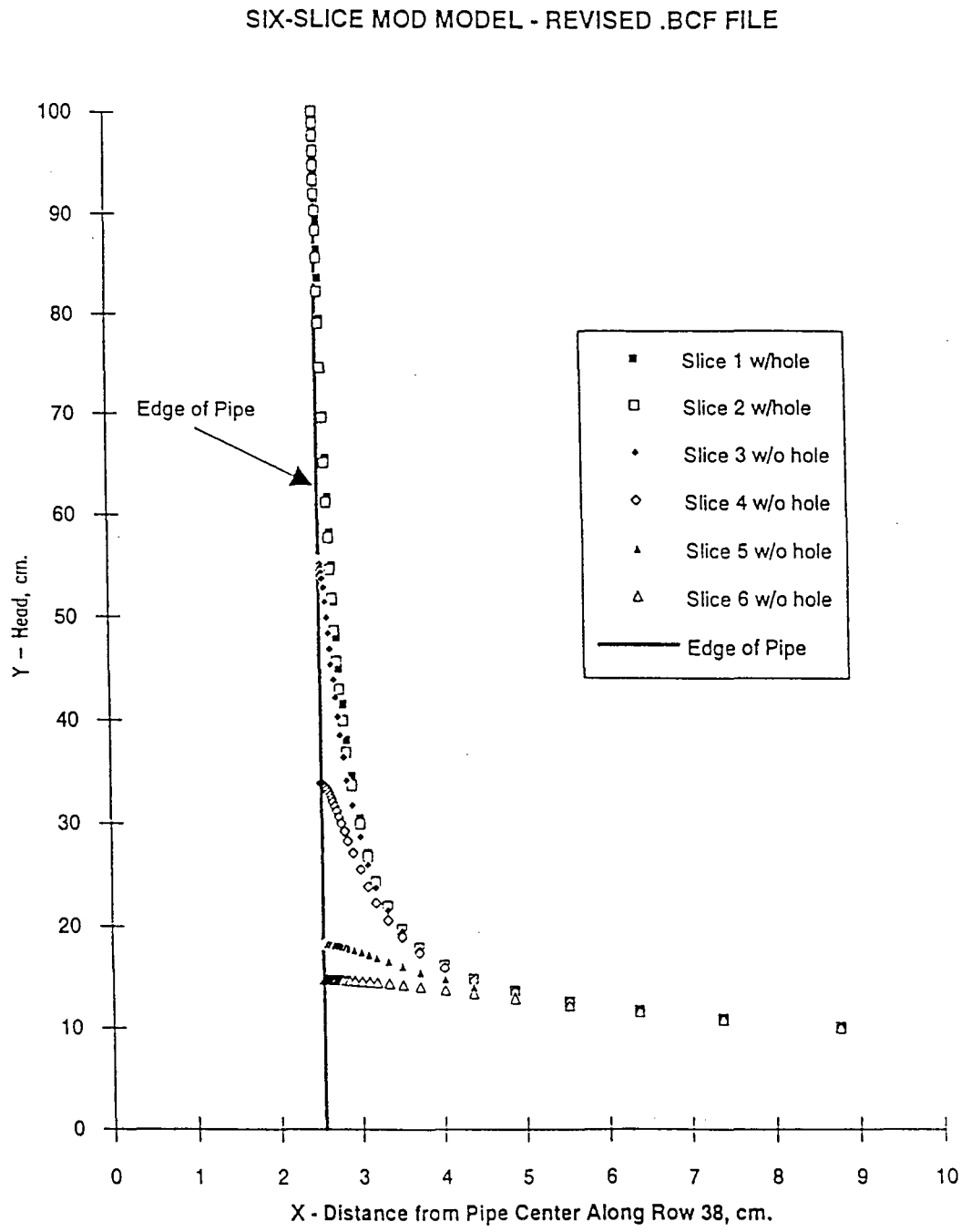

FIGURE 3.12

SEVEN-SLICE MOD MODEL - NEAR FIELD - SLICE SPACING AS IN FIG. 3.4, RUN 7A

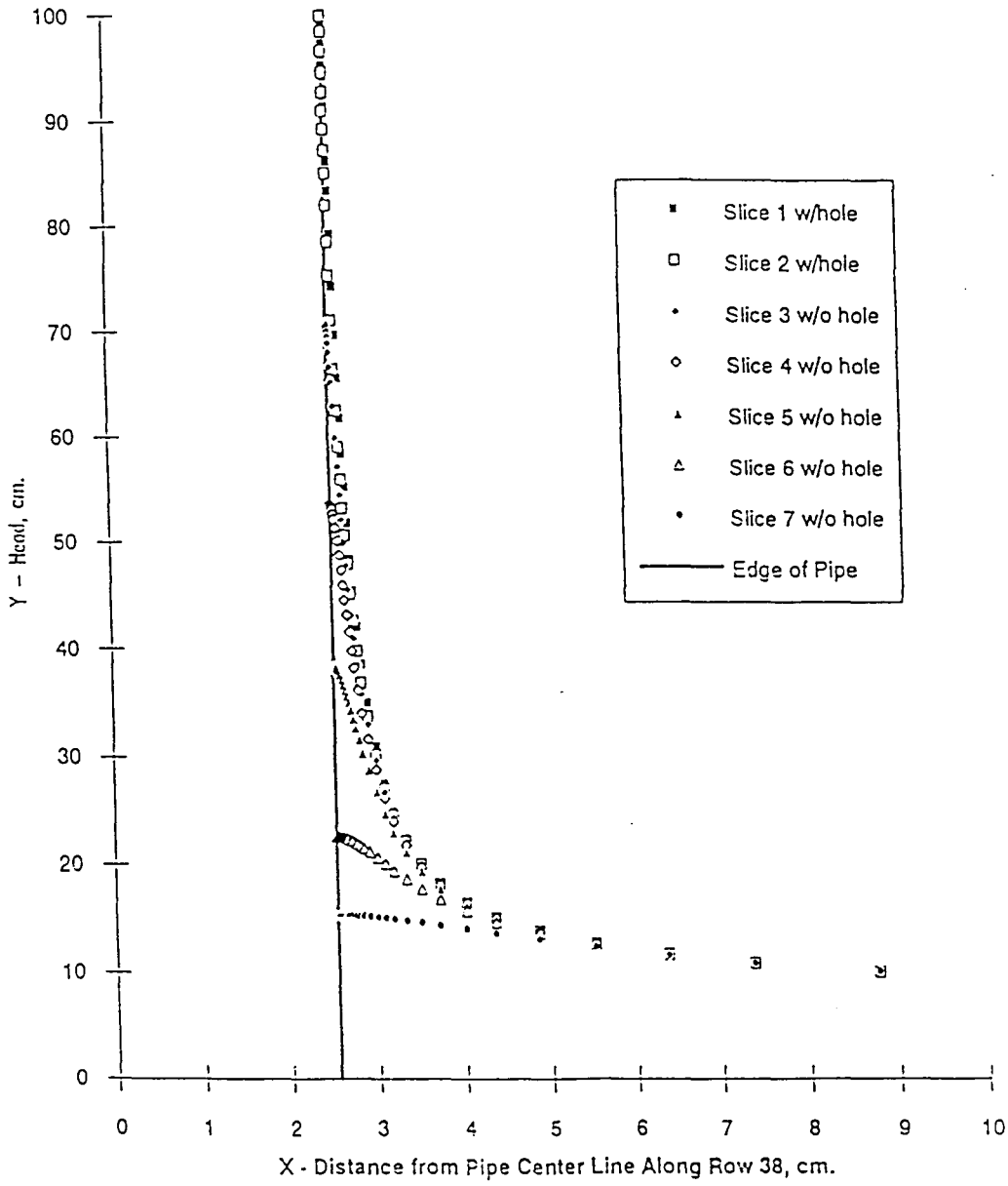

FIGURE 3.13

SEVEN SLICE MOD MODEL - NEAR FIELD - SLICE SPACING AS IN FIG. 3.4, RUN 7B

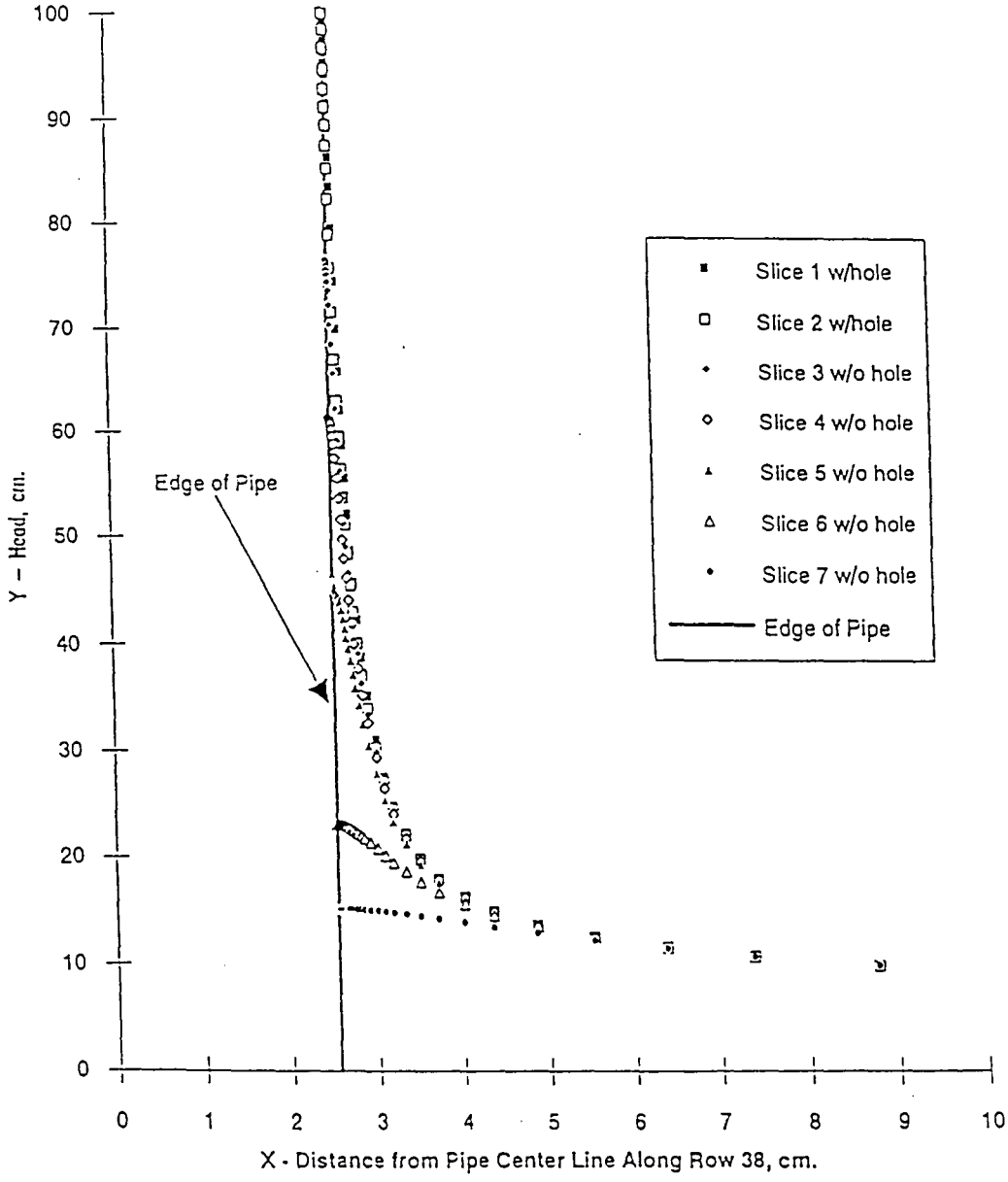

FIGURE 3.14

SEVEN SLICE MOD MODEL - FULL TANK - SLICE SPACING AS IN FIG. 3.4, RUN 7B

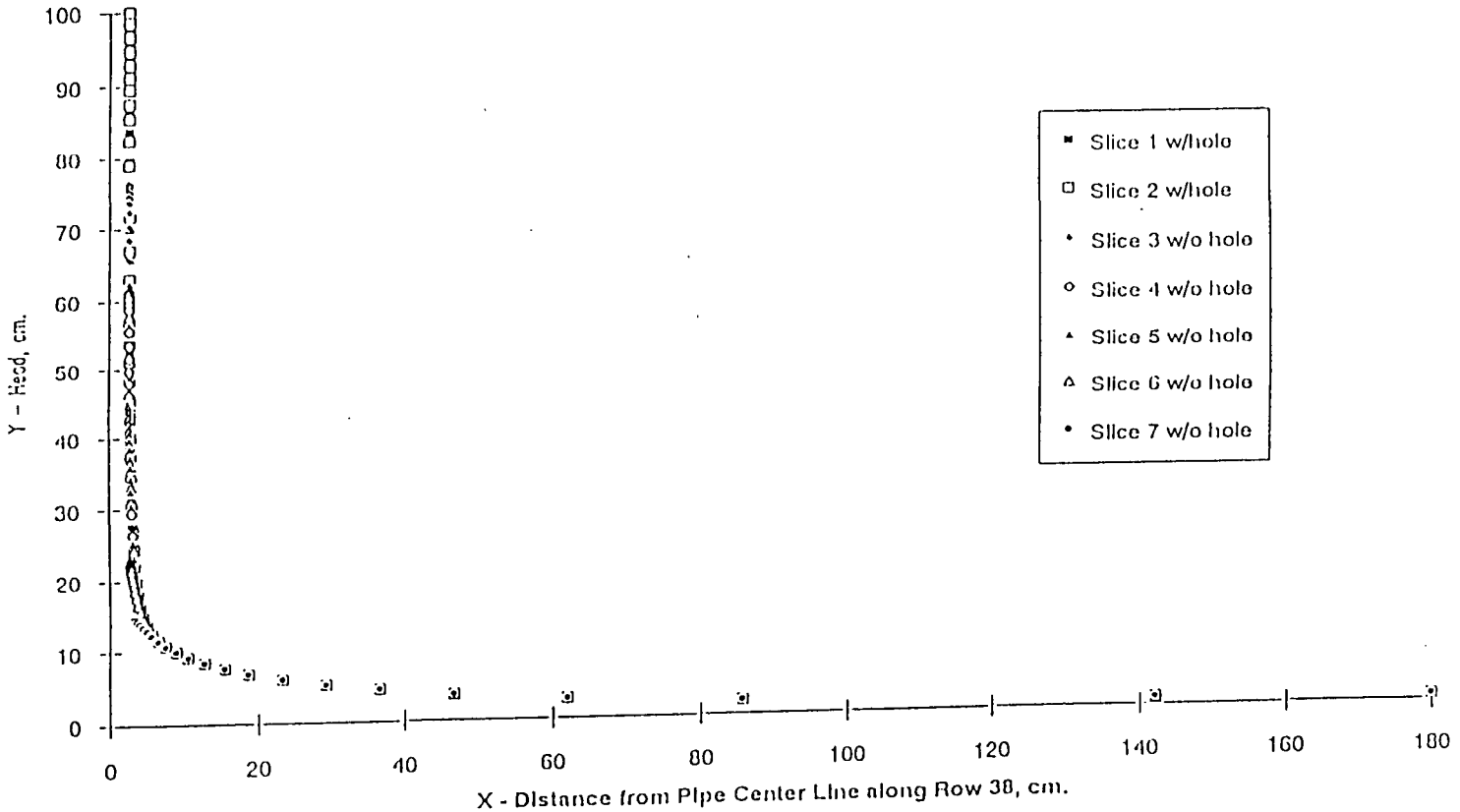

FIGURE 3.15

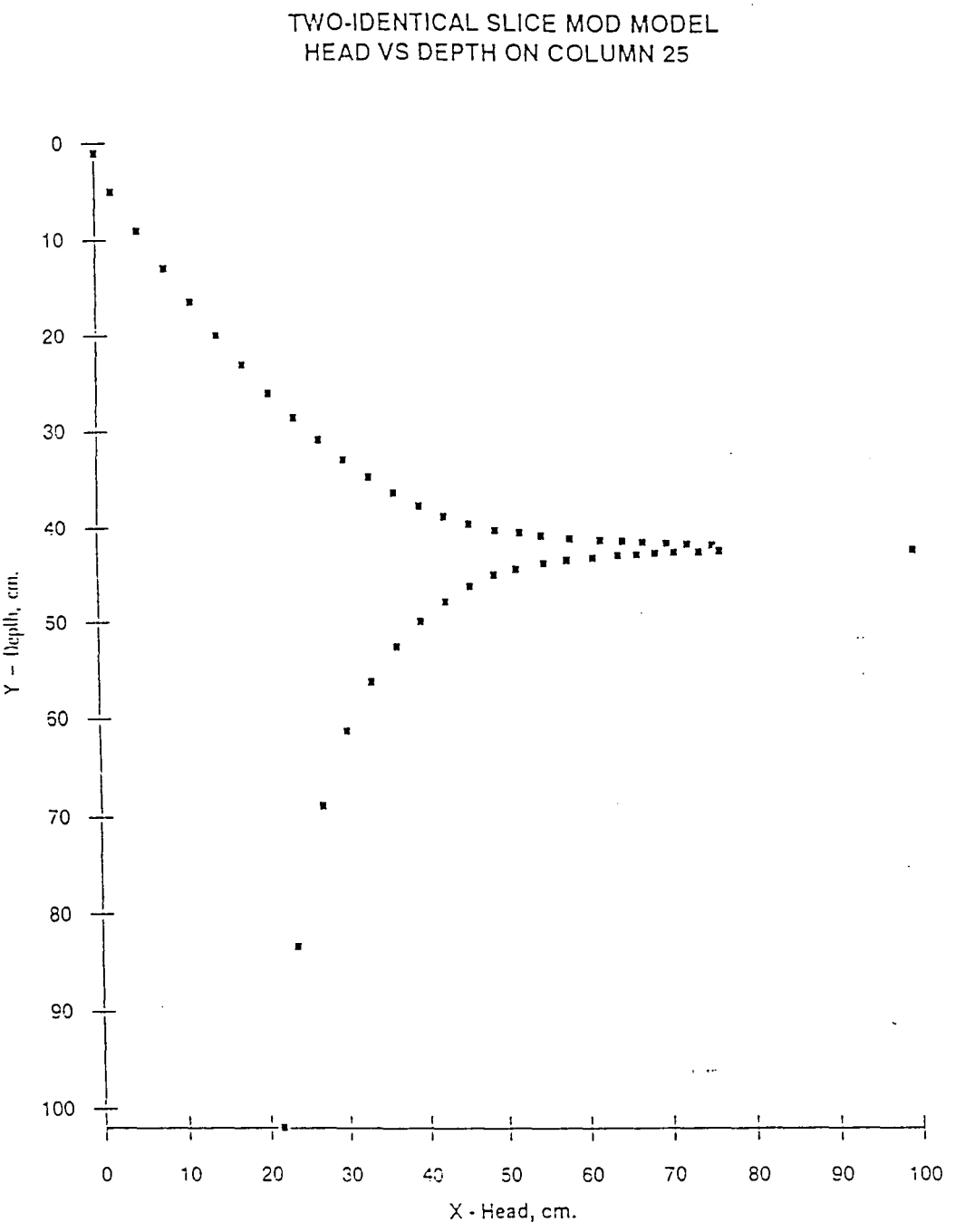
TWO-IDENTICAL SLICE MOD MODEL
HEAD VS DEPTH ON COLUMN 25
Y - Depth, cm.
0
10
20
30
40
50
60
70
80
90
100
X - Head, cm.

FIGURE 3.16

LA2YCUT2.XLS Chart 2

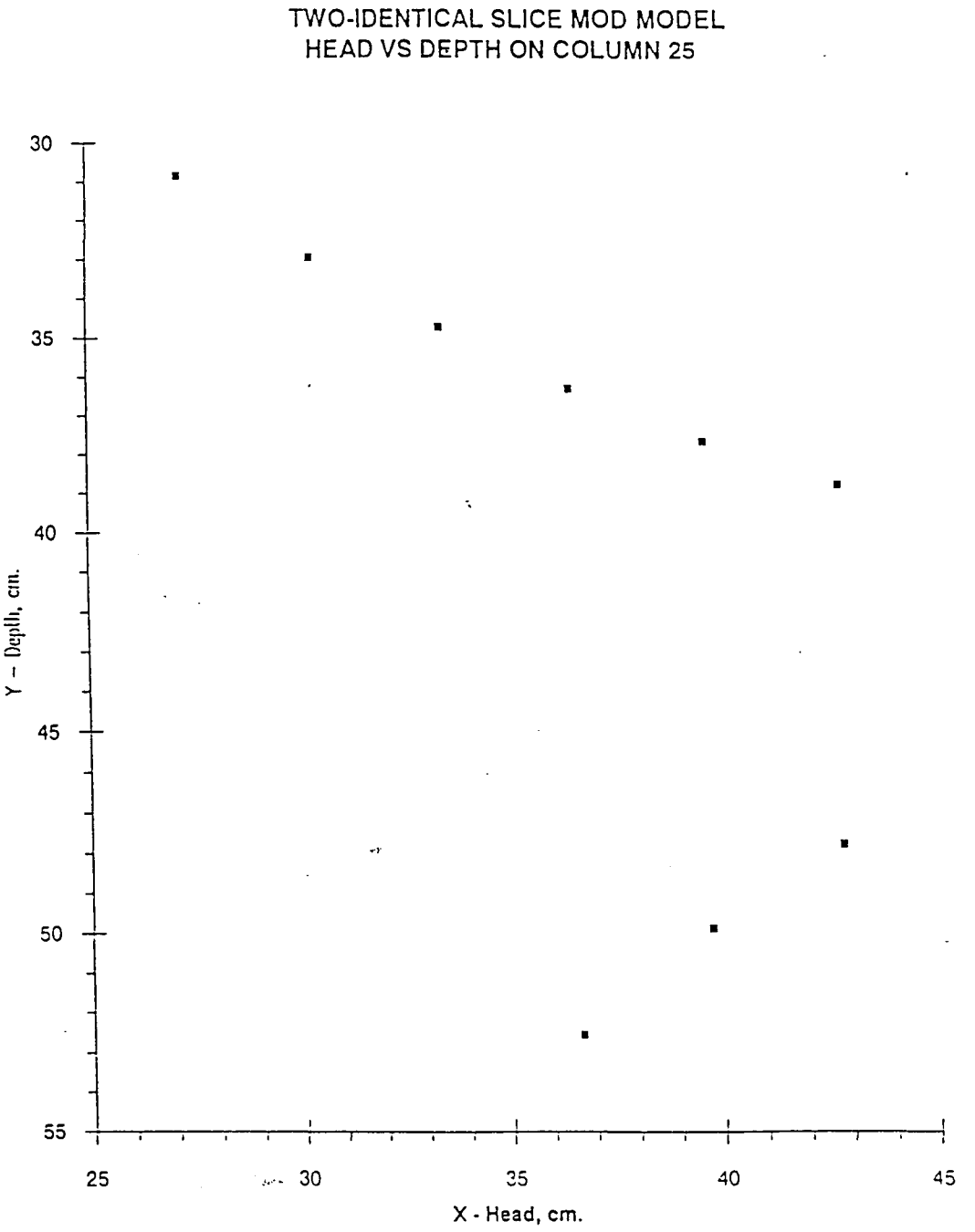

FIGURE 3.17

LAY2CUT2.XLS Chart 1

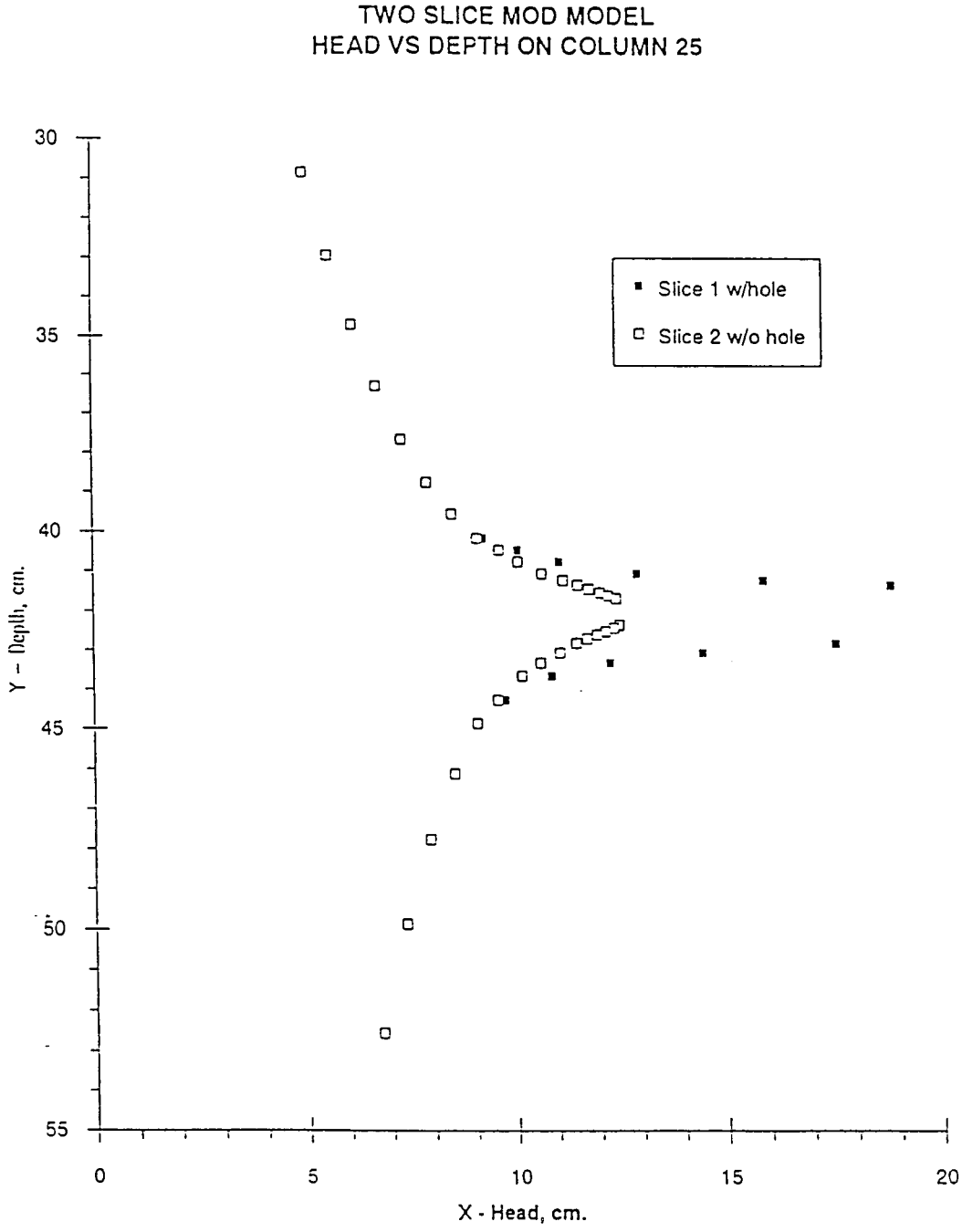

FIGURE 3.18

LAY3CUT2.XLS Chart 1

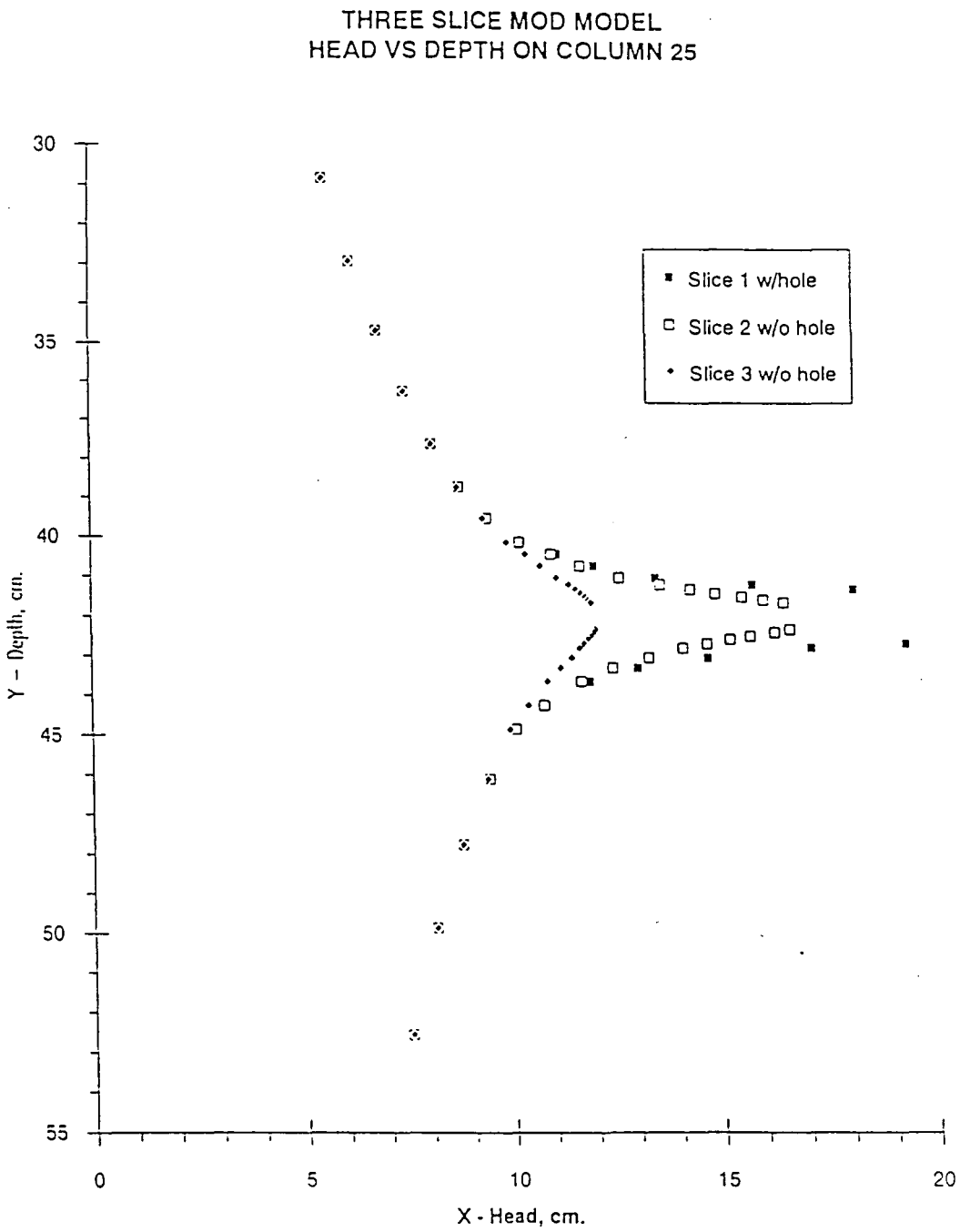

FIGURE 3.19

LAY4CUT2.XLS Chart 1

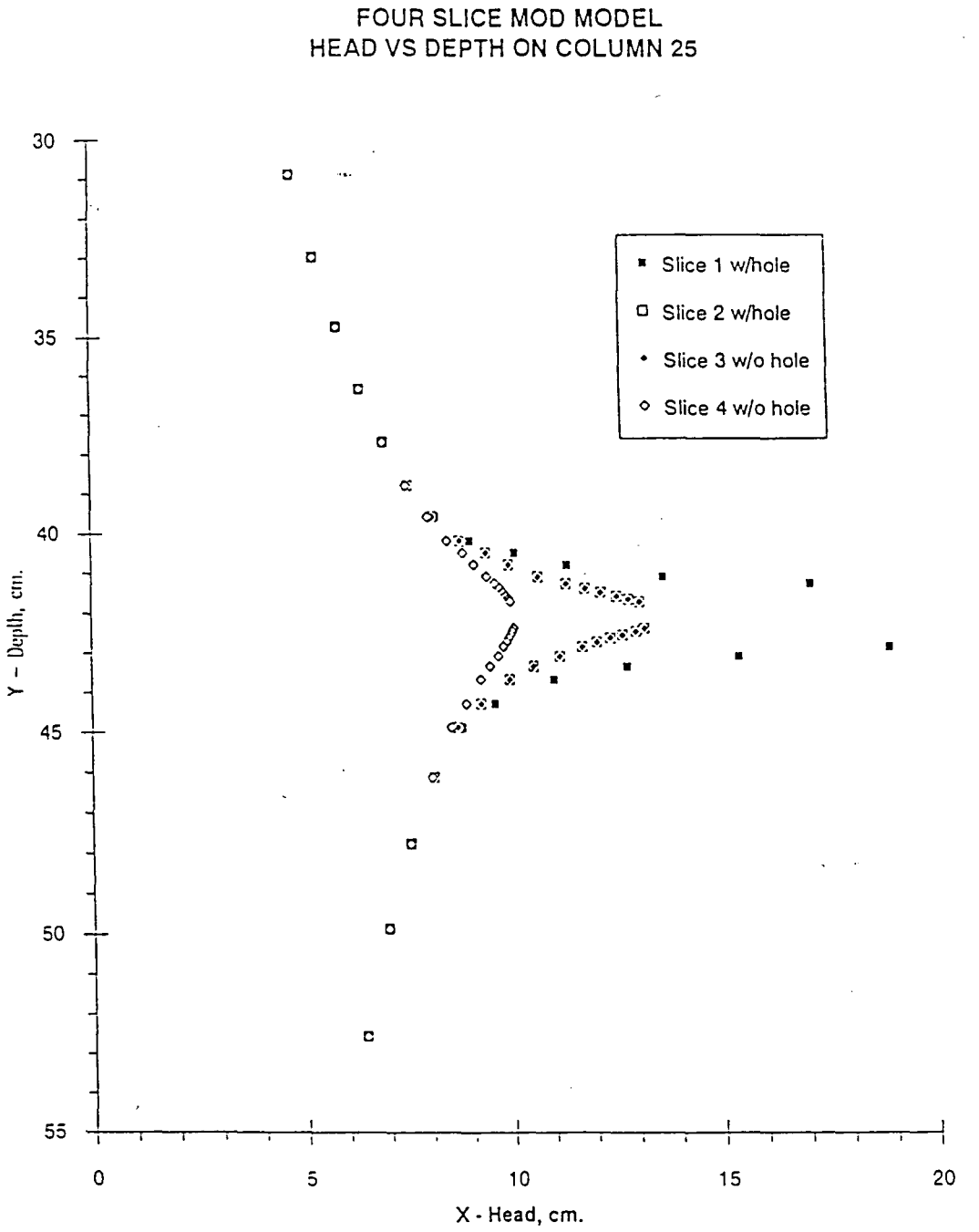

FIGURE 3.20

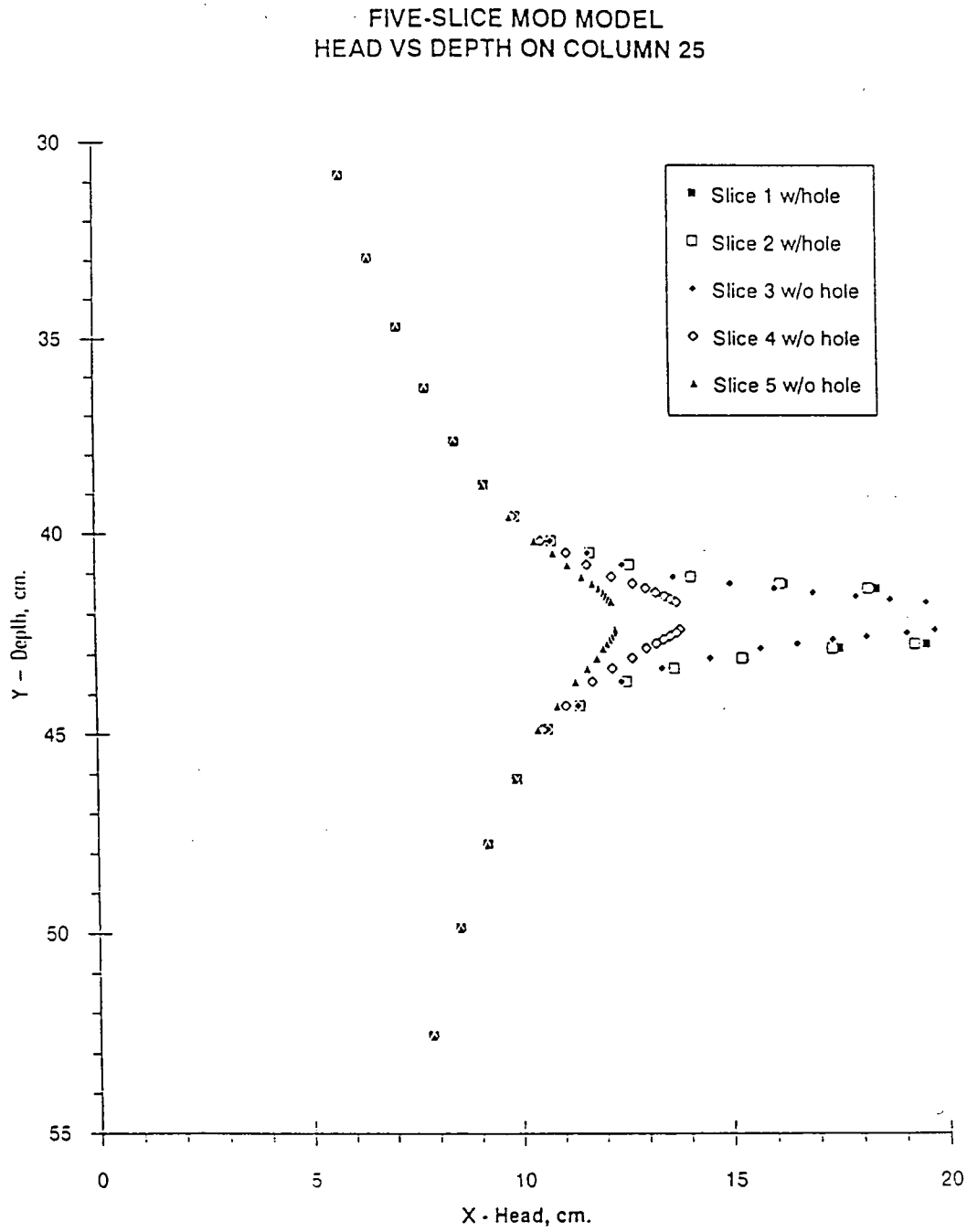
FIVE-SLICE MOD MODEL
HEAD VS DEPTH ON COLUMN 25
Slice 1 w/hole
Slice 2 w/hole
Slice 3 w/o hole
Slice 4 w/o hole
Slice 5 w/o hole
Y - Depth, cm.
30
35
40
45
50
55
0
5
10
15
20
X - Head, cm.

FIGURE 3.21

SIX-SLICE MOD MODEL
HEAD VS DEPTH ON COLUMN 25

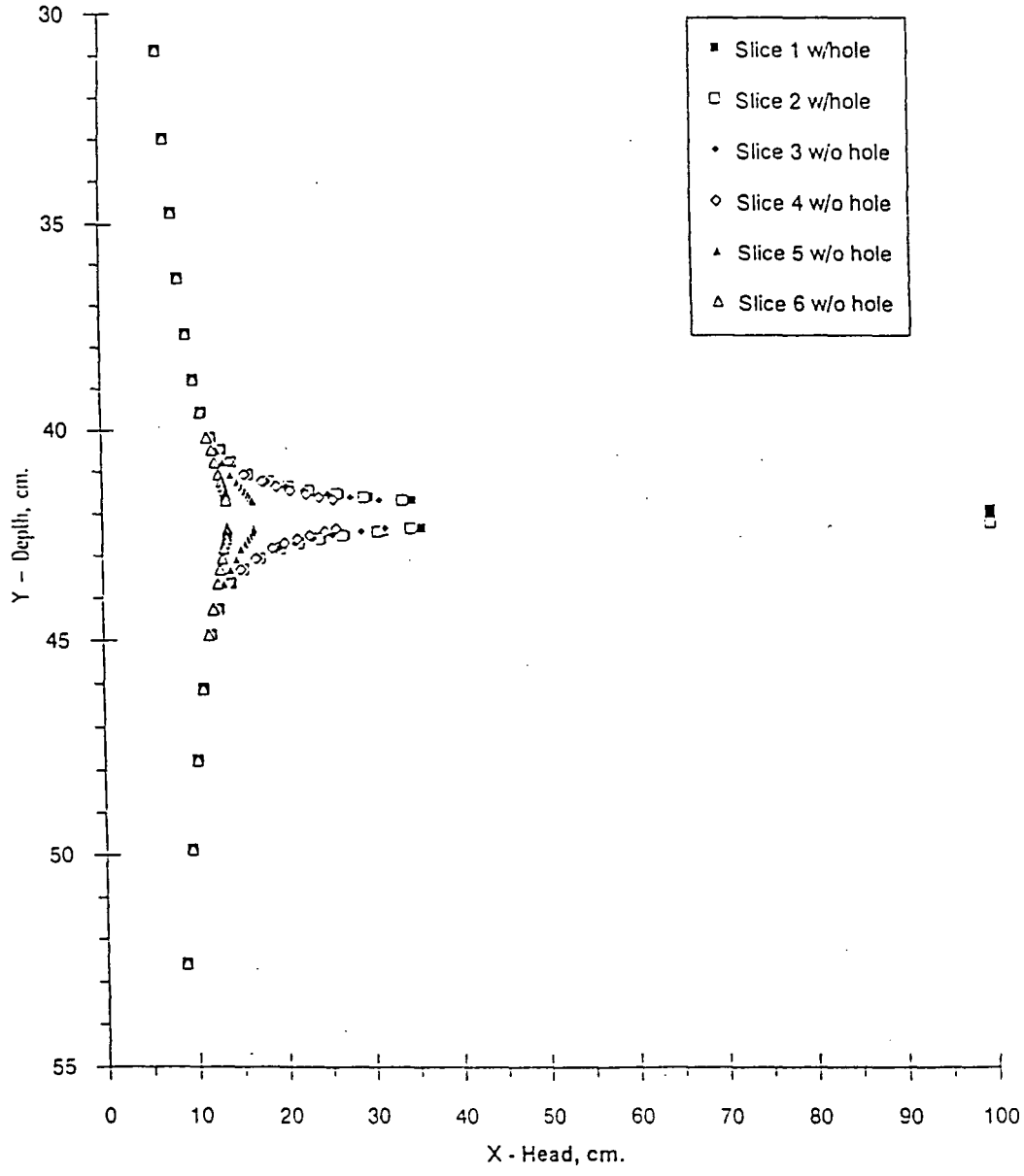

FIGURE 3.22

LA6CCUT1.XLS Chart 1

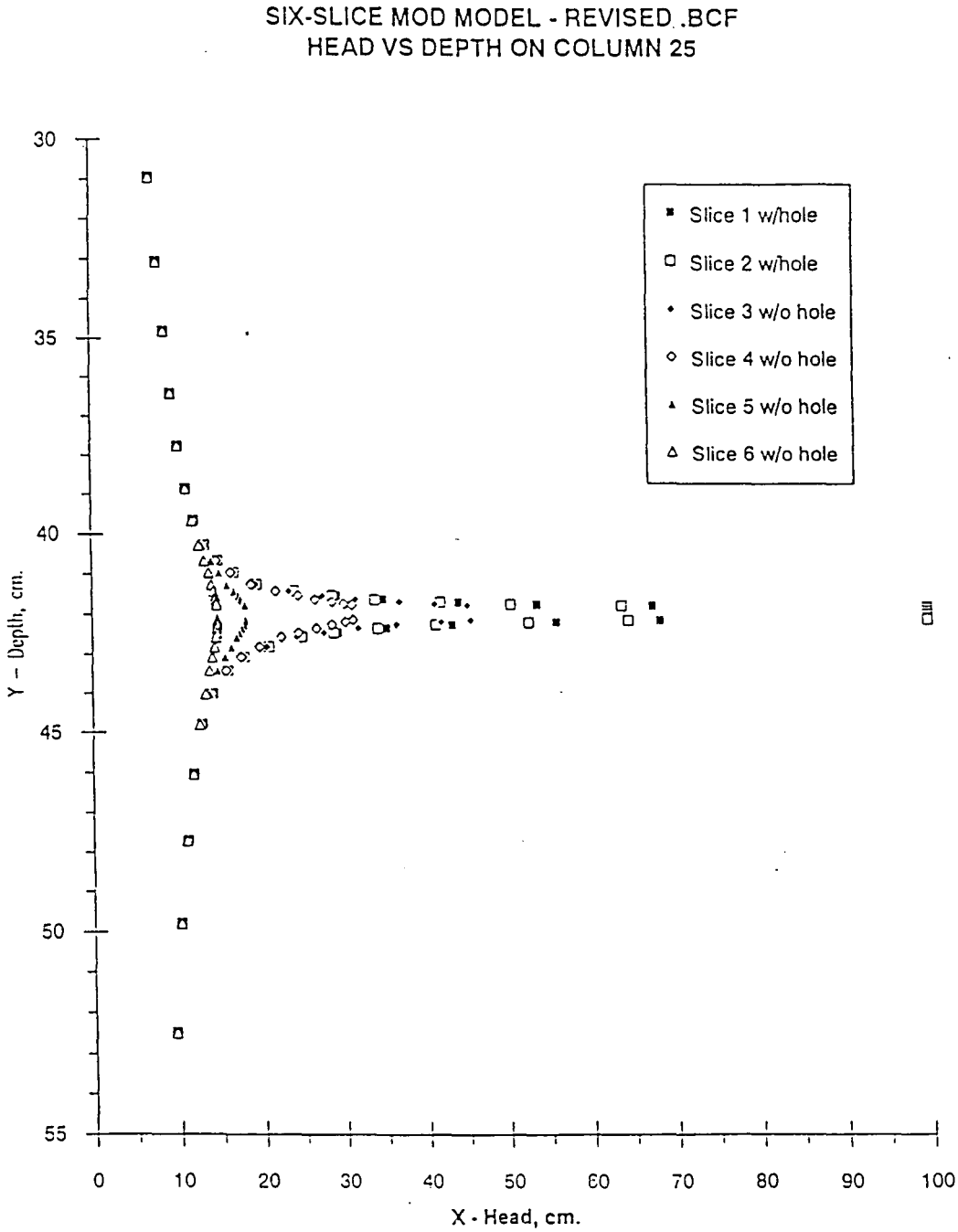

FIGURE 3.23

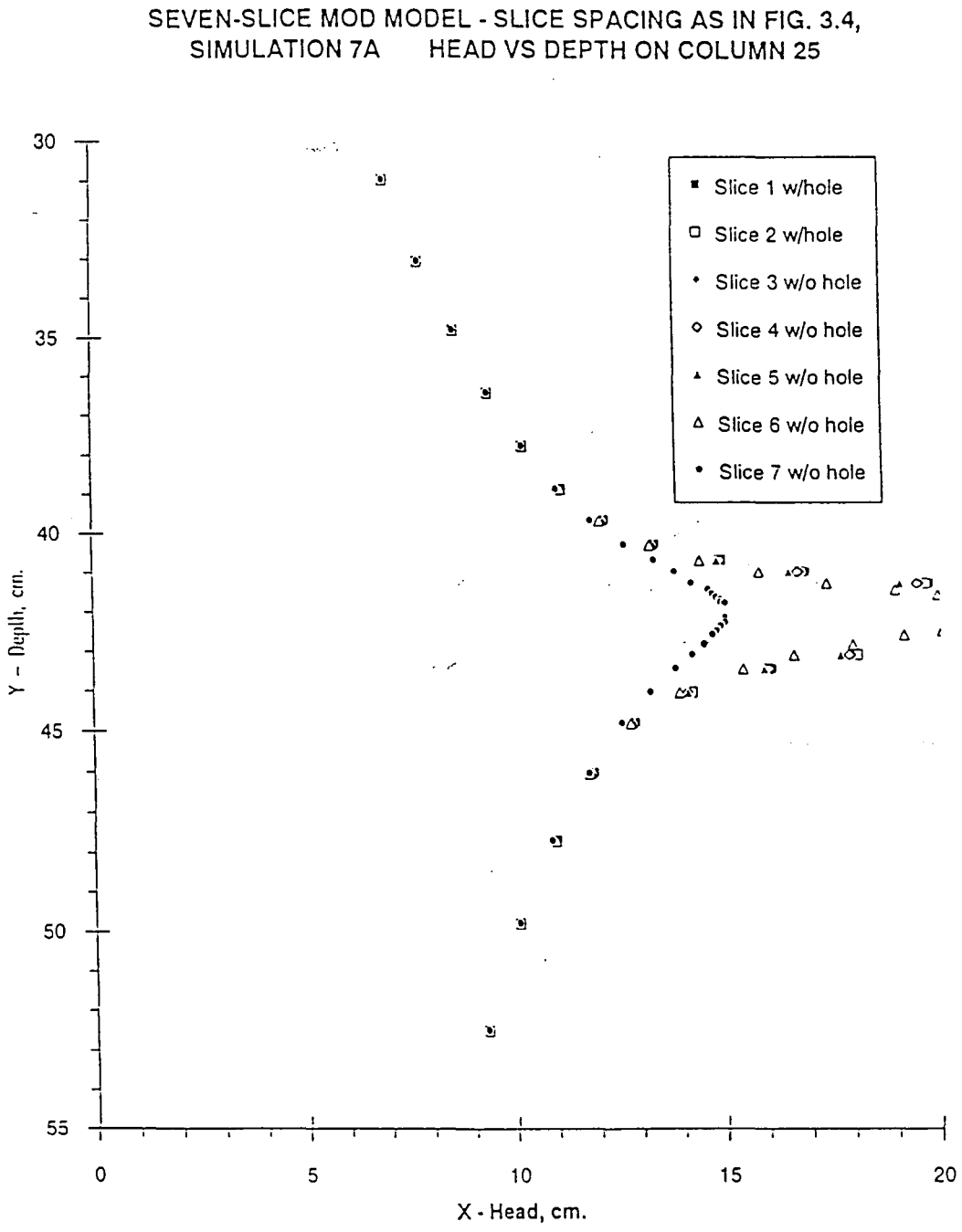
SEVEN-SLICE MOD MODEL - SLICE SPACING AS IN FIG. 3.4,
SIMULATION 7A HEAD VS DEPTH ON COLUMN 25
Slice 1 w/hole
Slice 2 w/hole
Slice 3 w/o hole
Slice 4 w/o hole
Slice 5 w/o hole
Slice 6 w/o hole
Slice 7 w/o hole
Y - Depth, cm.
30
35
40
45
50
55
0
5
10
15
20
X - Head, cm.

FIGURE 3.24

LAY7CUT3.XLS Chart 2

SEVEN-SLICE MOD MODEL - SLICE SPACING AS IN FIG. 3.4,
SIMULATION 7A HEAD VS DEPTH ON COLUMN 25
EXPANDED X-DOMAIN

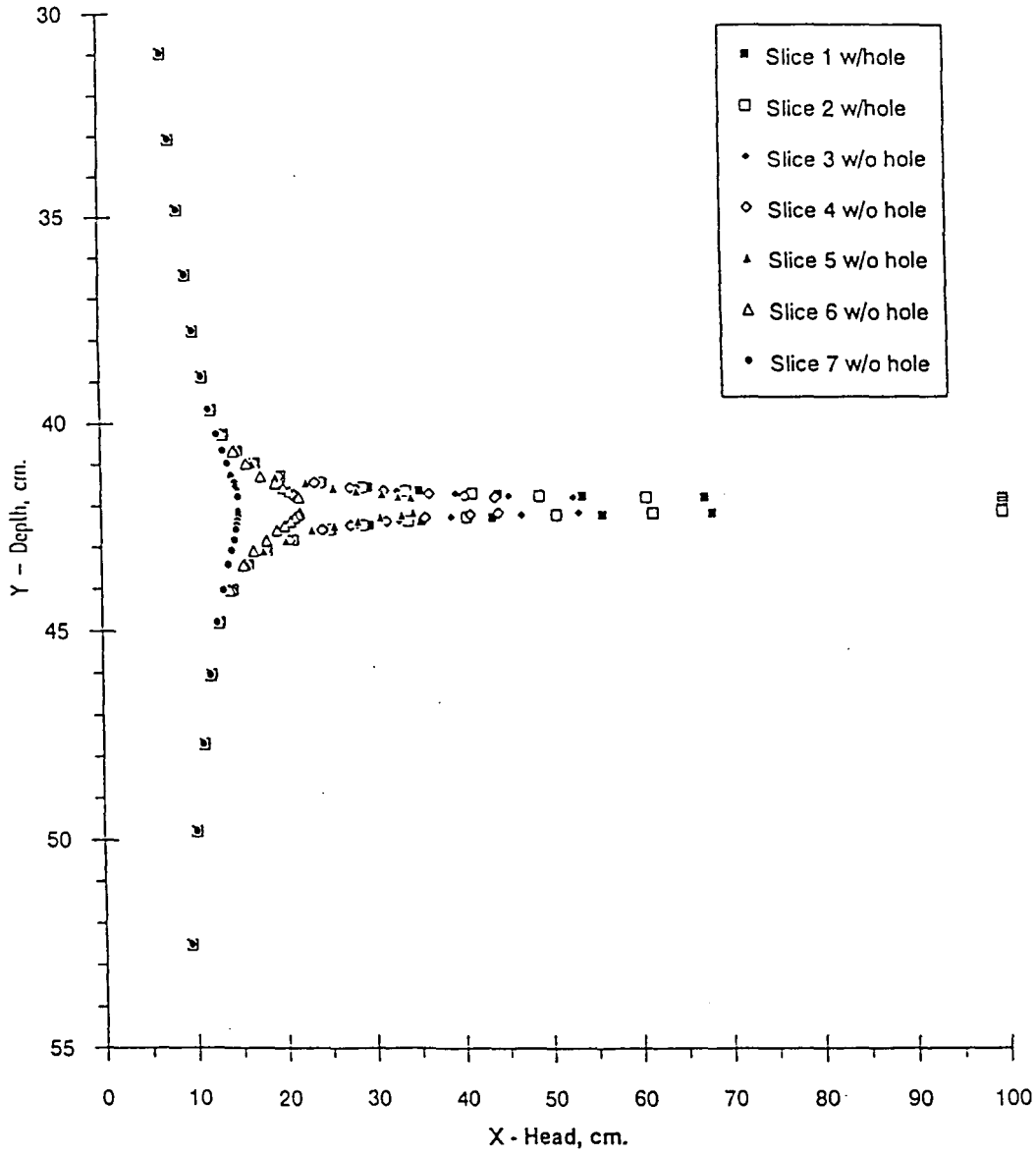

FIGURE 3.24A

SEVEN-SLICE MOD MODEL, NEAR FIELD - SLICE SPACING AS IN FIG. 3.4, RUN 7B HEAD VS DEPTH ON COLUMN 25

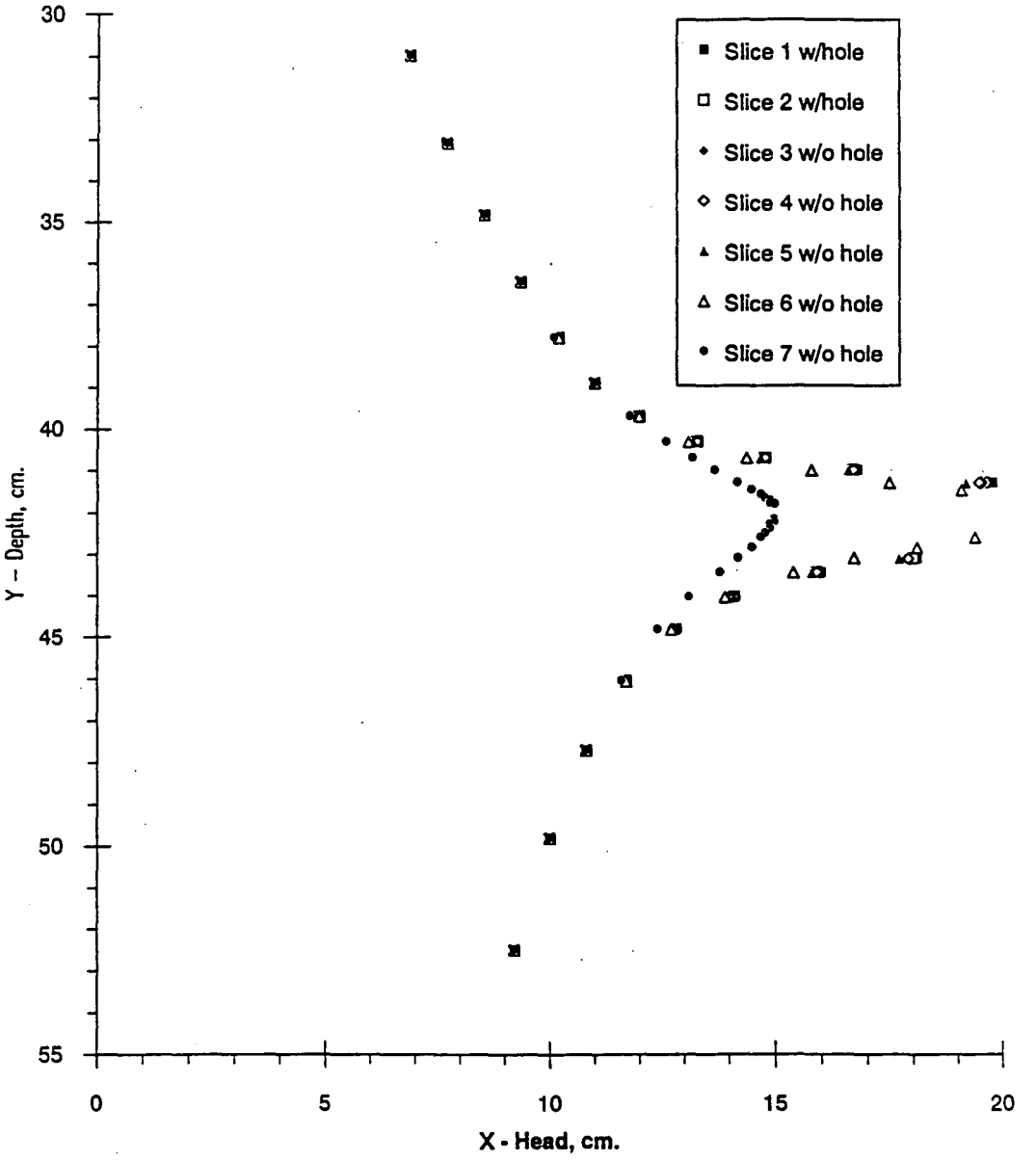

FIGURE 3.25

SEVEN-SLICE MOD MODEL, NEAR FIELD - SLICE SPACING AS IN FIG. 3.4, RUN 7B HEAD VS DEPTH ON COLUMN 25 EXPANDED X-DOMAIN

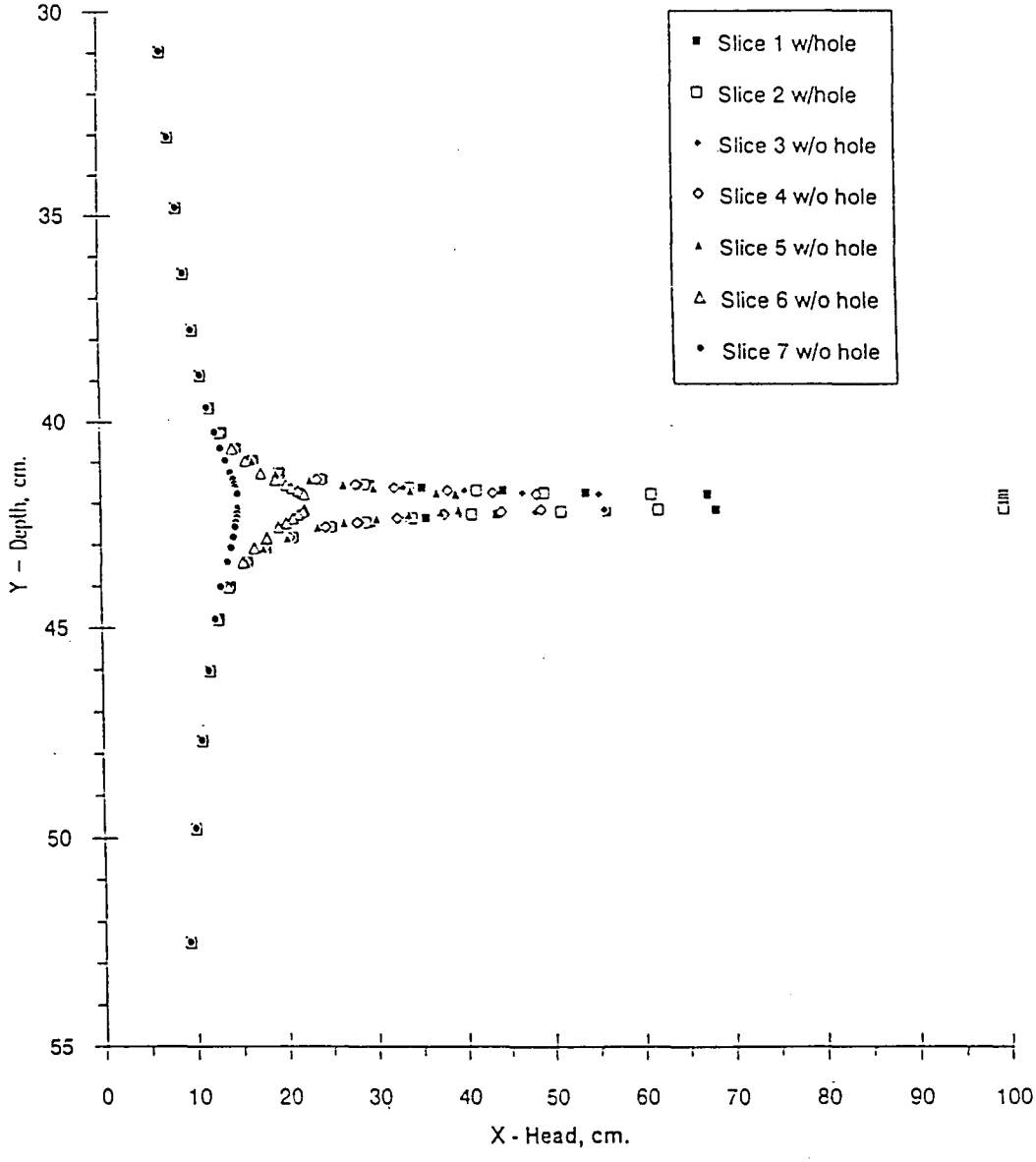

FIGURE 3.25A

LA7BCUT2.XLS Chart 2

SEVEN-SLICE MOD MODEL, FULL TANK - SLICE SPACING AS IN FIG. 3.4, RUN 7B HEAD VS DEPTH ON COLUMN 25

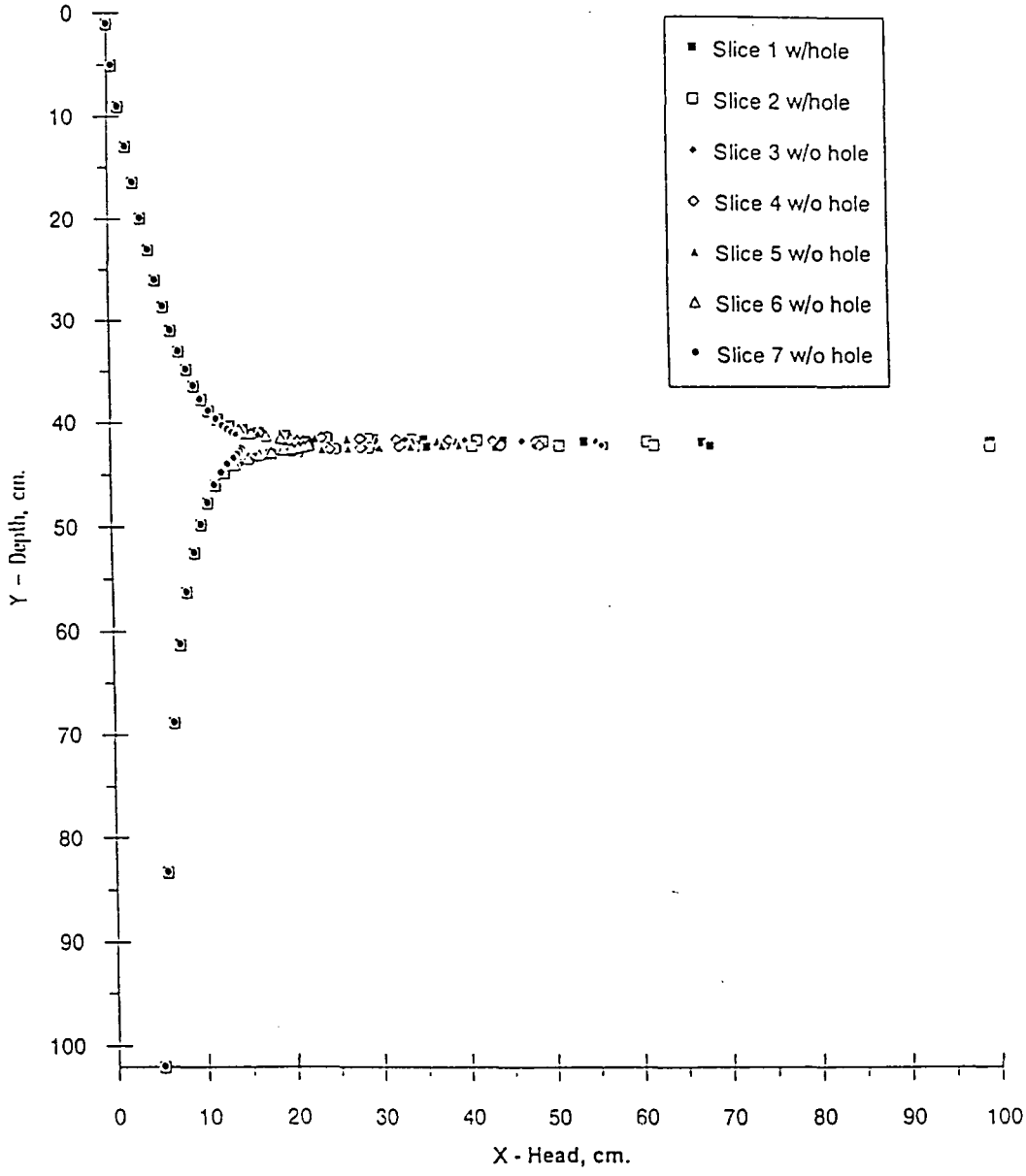

FIGURE 3.26

SEVEN-SLICE MOD MODEL - RIBBON PLOT

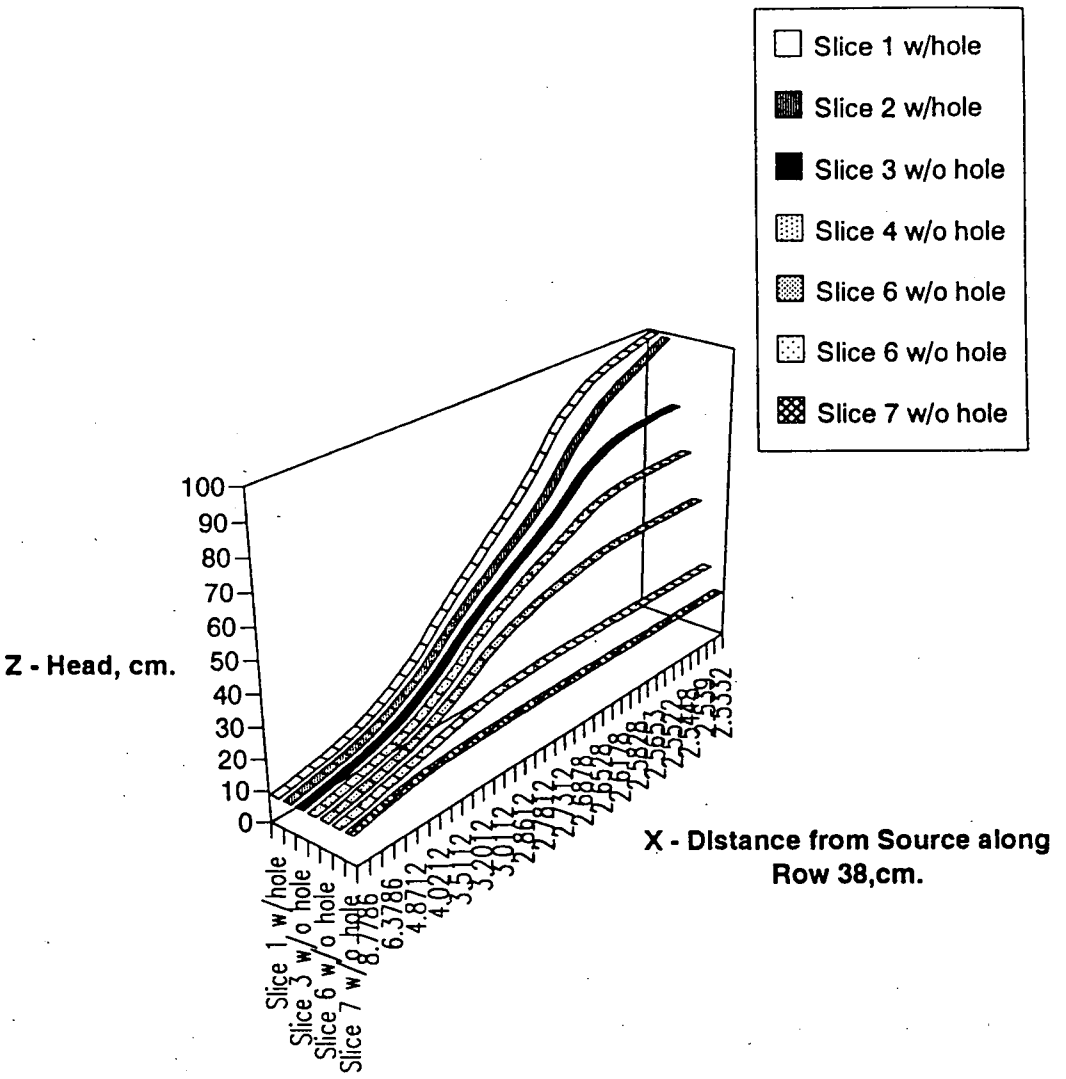

FIGURE 3.27

TWO-IDENTICAL SLICE (W/SMALLER SLOT) MOD MODEL HEAD VS DISTANCE ALONG ROW 38, FULL TANK

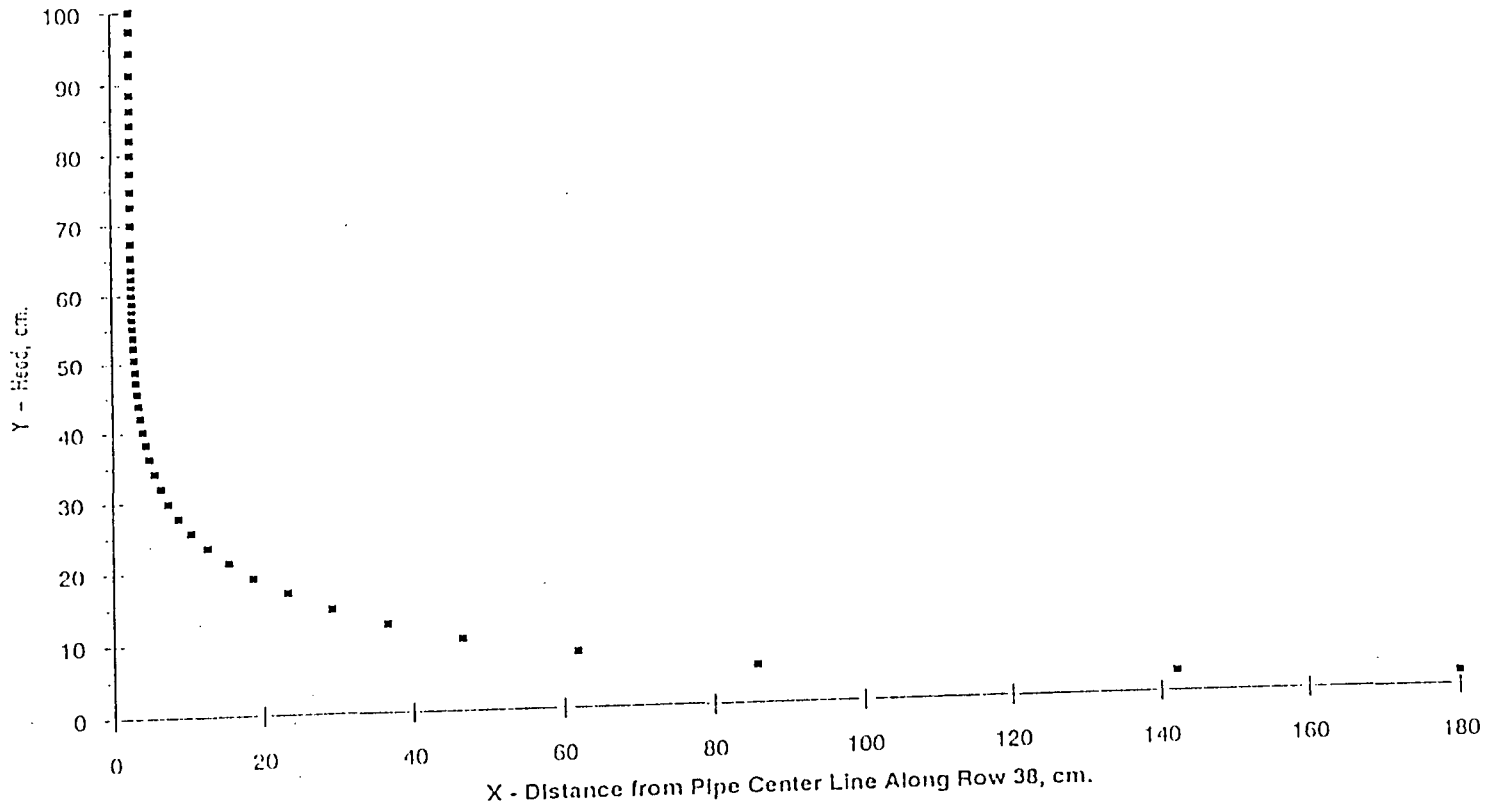

FIGURE 3.28

TWO-IDENTICAL SLICE (W/SMALLER SLOT) MOD MODEL HEAD
VS DISTANCE ALONG ROW 38, NEAR FIELD

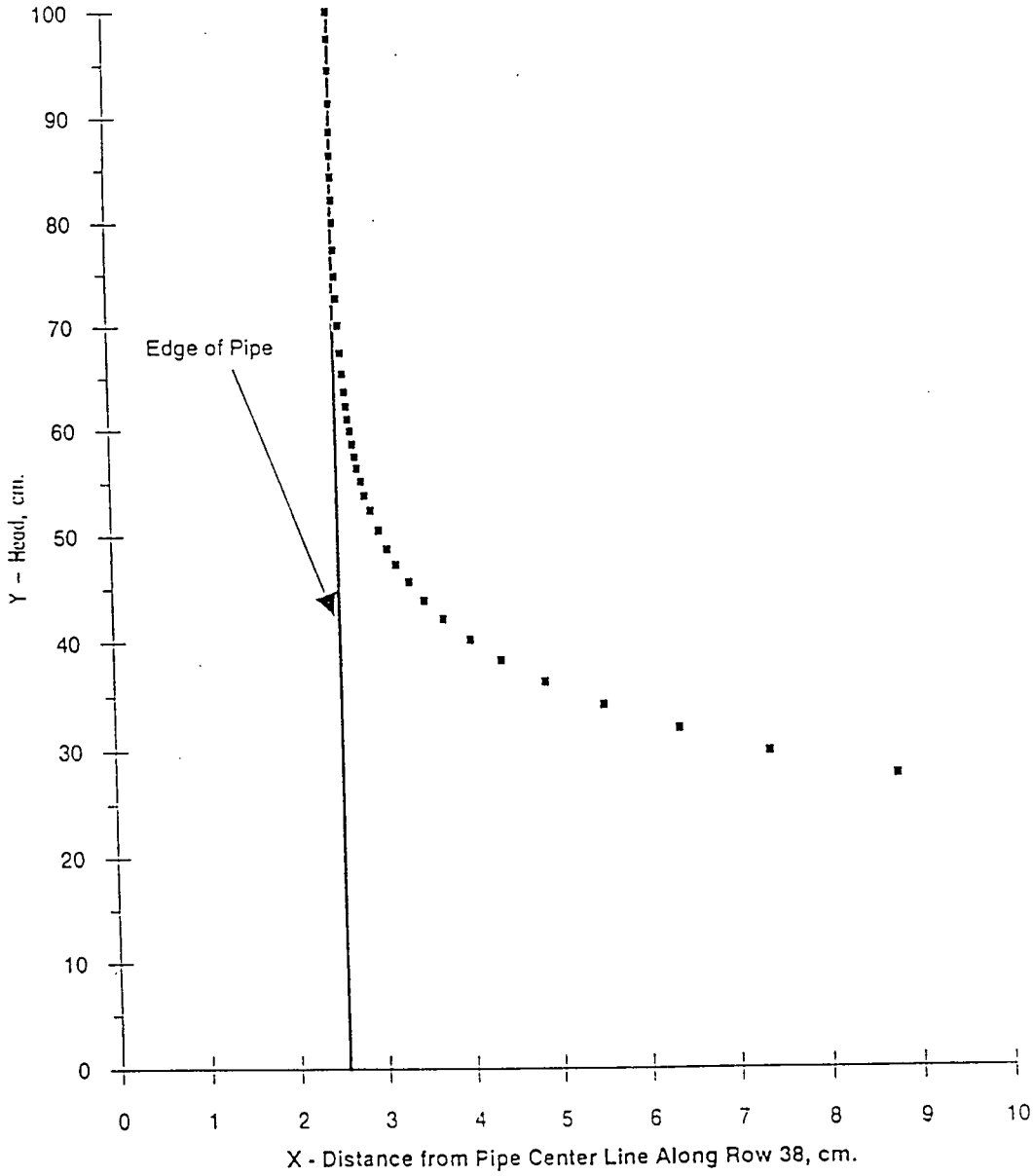

FIGURE 3.29

TWO-IDENTICAL SLICE MOD MODEL (W/SMALLER SLOT) HEAD VS DEPTH ON COLUMN 25, FULL TANK

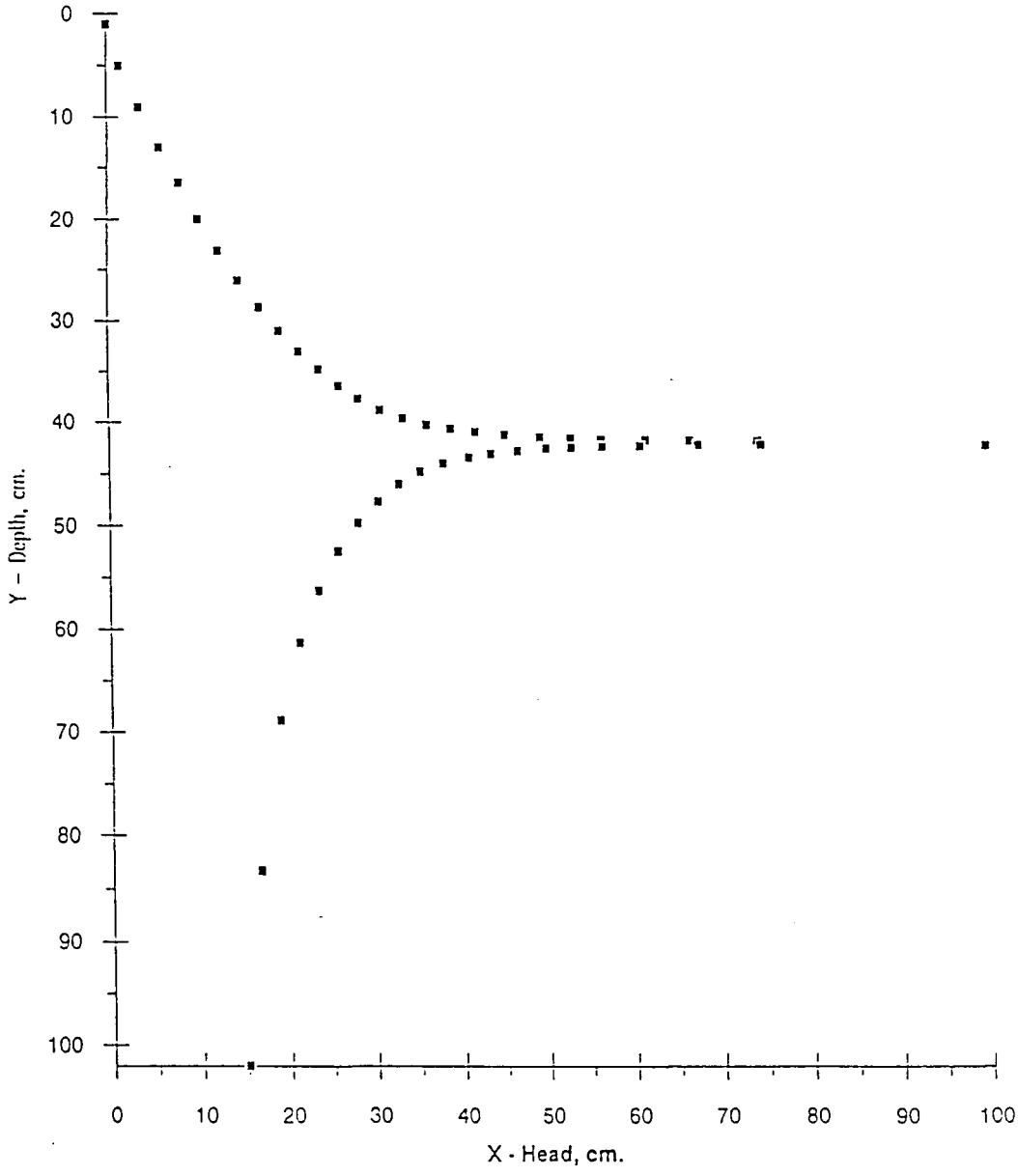

FIGURE 3.30

TWO-IDENTICAL SLICE MOD MODEL (W/SMALLER SLOT) HEAD
VS DEPTH ON COLUMN 25, NEAR FIELD

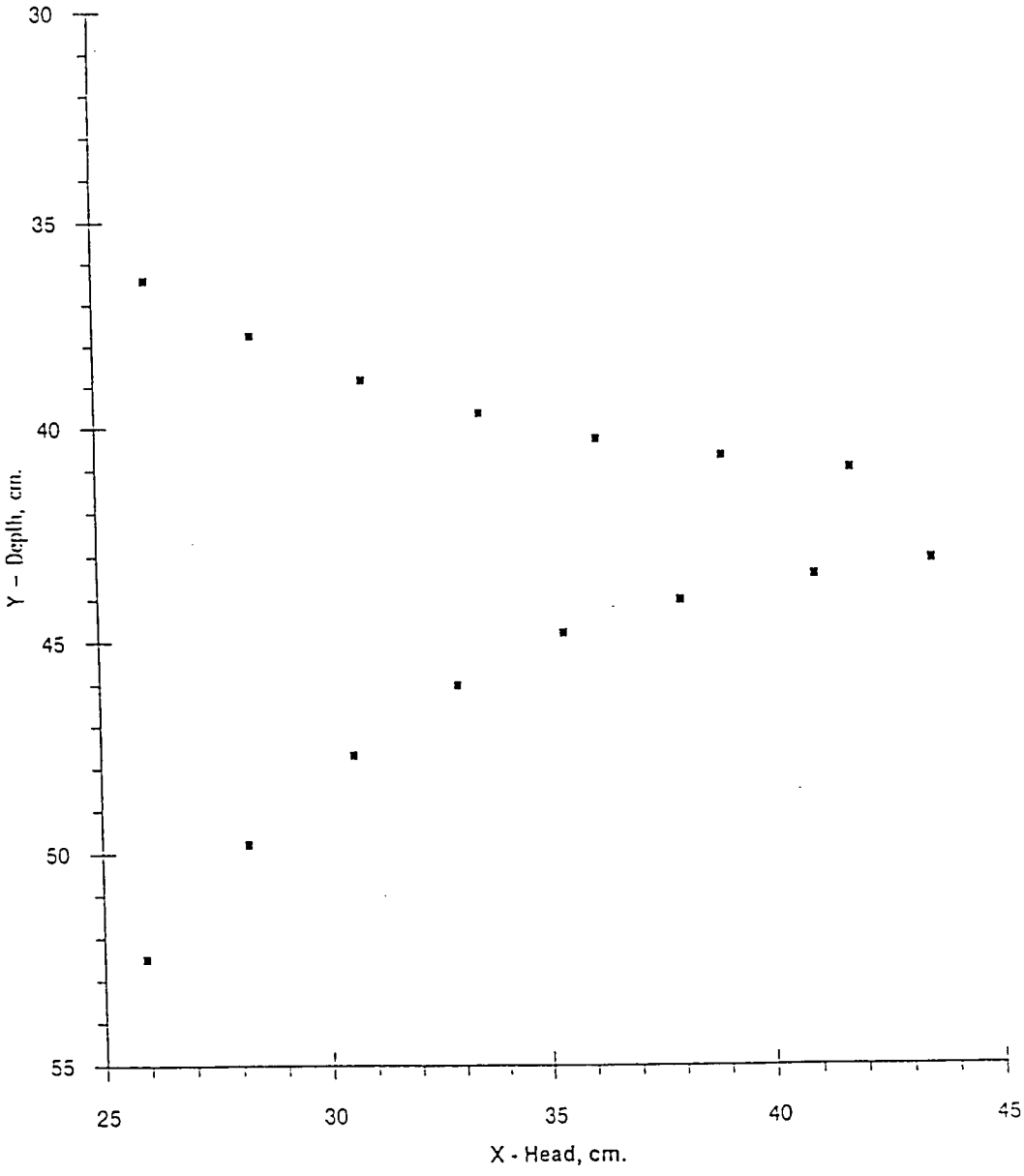

FIGURE 3.31

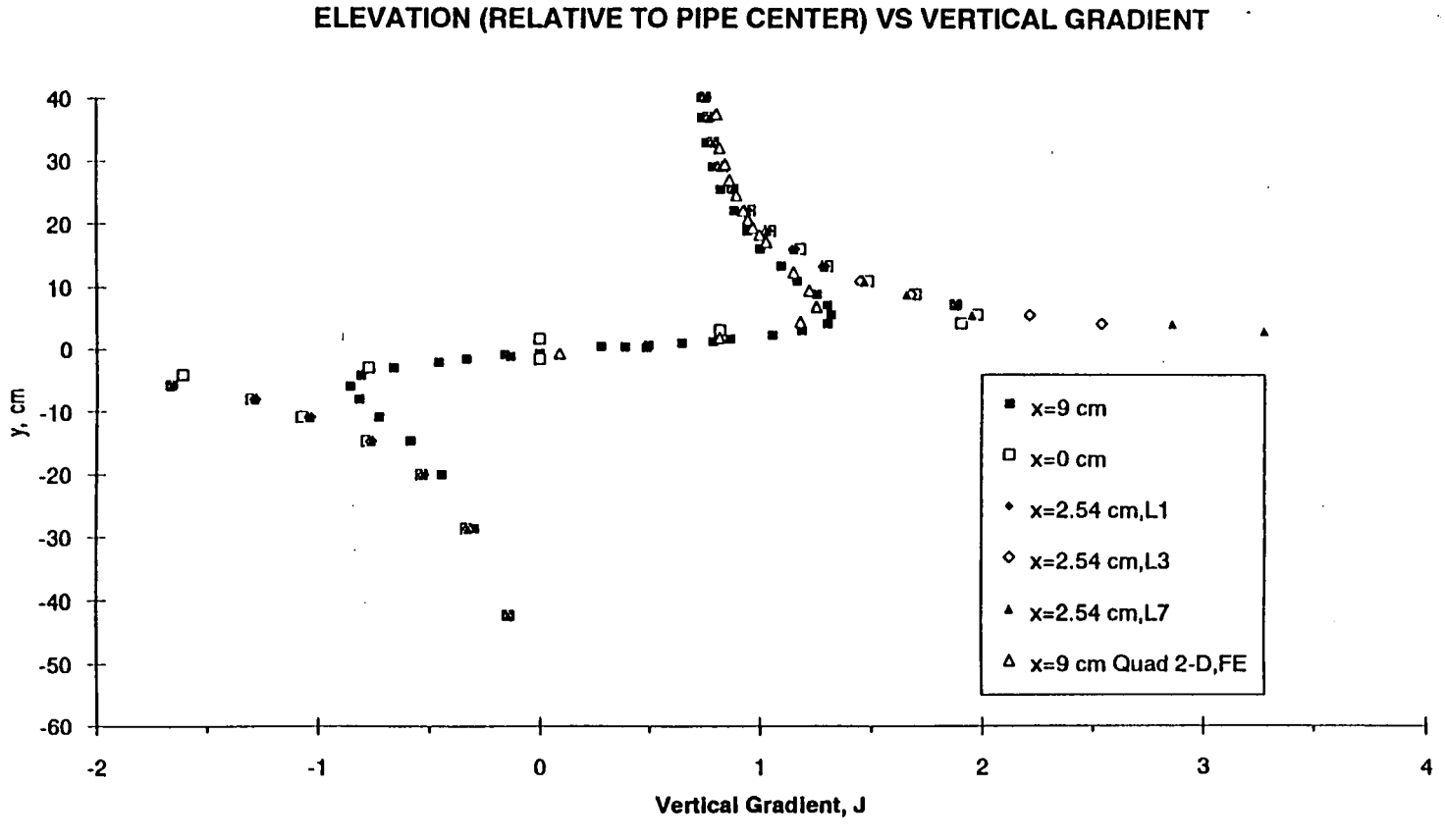
ELEVATION (RELATIVE TO PIPE CENTER) VS VERTICAL GRADIENT
y, cm
40
30
20
10
0
-10
-20
-30
-40
-50
-60
-2
-1
0
1
2
3
4
Vertical Gradient, J
x=9 cm
x=0 cm
x=2.54 cm,L1
x=2.54 cm,L3
x=2.54 cm,L7
x=9 cm Quad 2-D,FE

FIGURE 3.32

L7C062.XLS Chart 21

ELEVATION (RELATIVE TO PIPE CENTER) VS VERTICAL GRADIENT COMPARISON BETWEEN MOD AND FINITE ELEMENT RESULTS

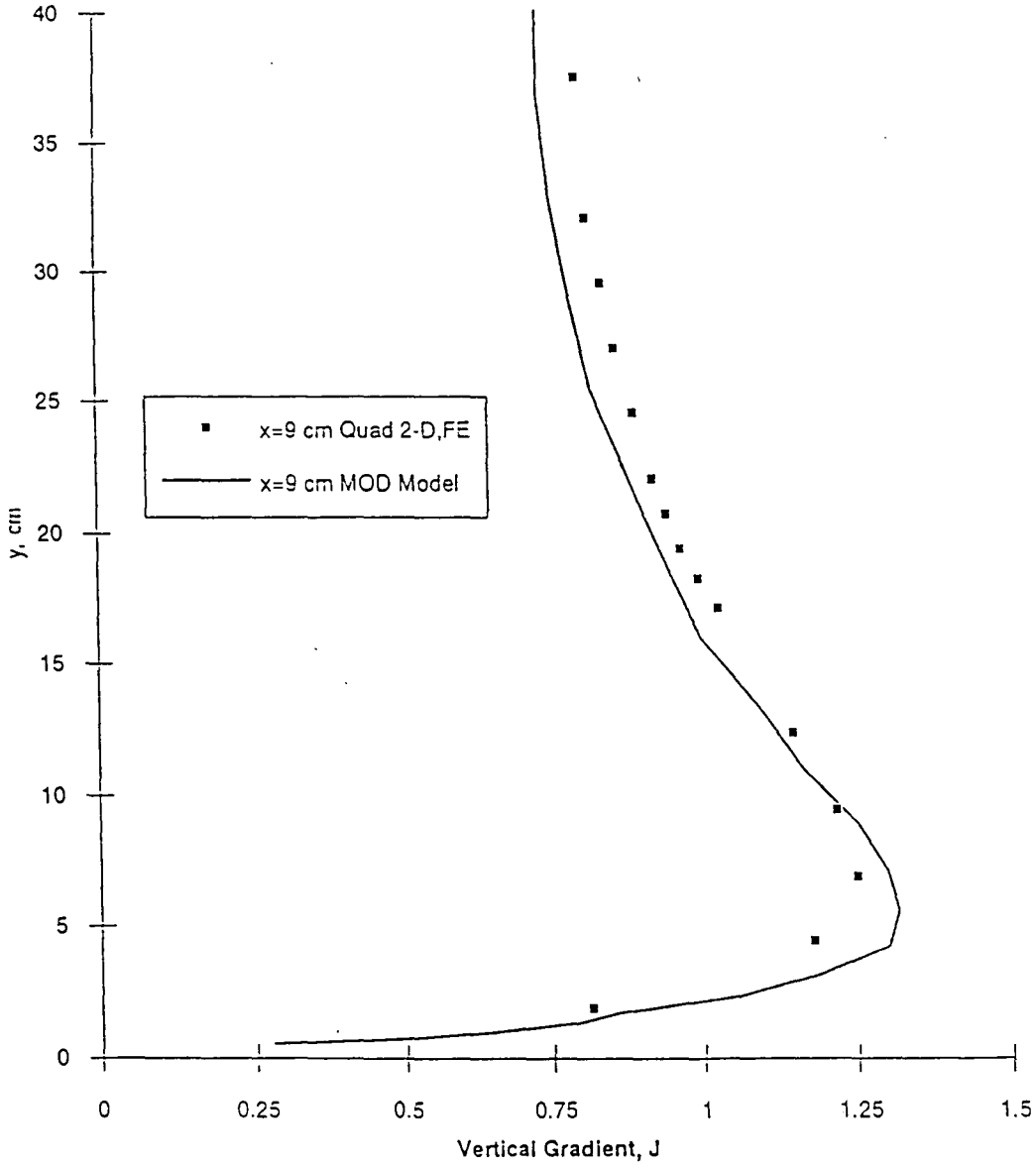

FIGURE 3.33

FIGURE 3.34

HYDRAULIC HEAD PLOT

LAYER 1 OF 7

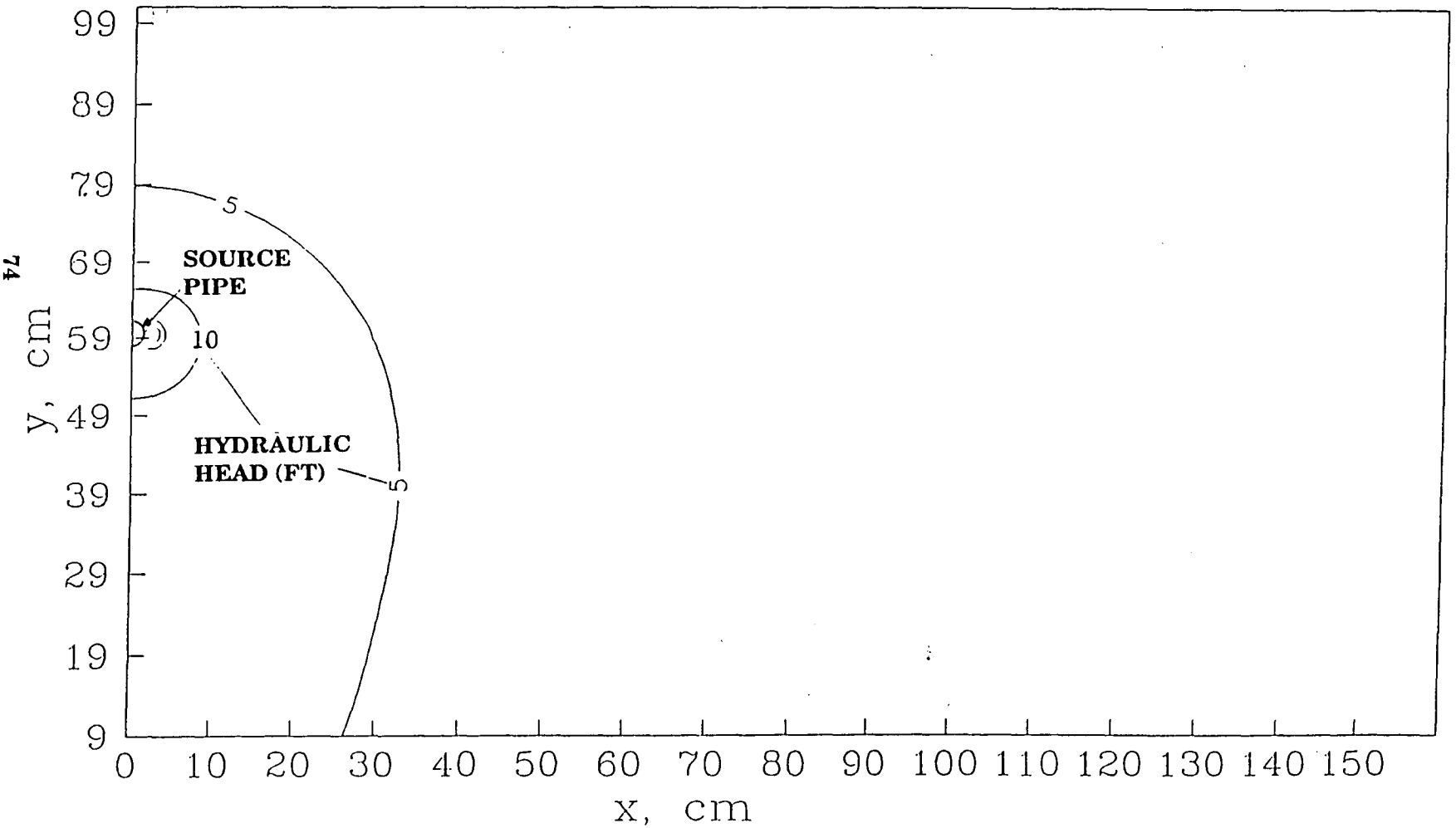

REFERENCES

Bear, J. 1972. Dynamics of Fluids in Porous Media, Elsevier, New York, N.Y.

Cleasby, J.L., and Fan, K.S., "Predicting Fluidization and Expansion of Filter Media". Journal of Environmental Engineering Division, ASCE, Vol. 107, No. EE3, (1981), 455-461.

Clifford, J.T., Weisman, R.N., Lennon, G.P. 1989. Slurry Removal from the Fluidized Region of an Unbounded Domain: An Experimental Study. Masters Thesis, Lehigh University, Bethlehem, PA.

Freeze, R.A., and Cherry, J.A. 1979. Groundwater. Prentice-Hall, Inc., N.J.

Hansen, P.J. 1991. Computer Automated Development of Groundwater Remedial Alternatives. Masters Thesis, Lehigh University, Bethlehem, PA.

Kopaskie, K.A. 1991. 2-D Quadratic Finite Element Modeling of Incipient Fluidization: Simulation of Porous Media Flow. Lehigh University, Bethlehem, PA.

Lennon, G.P., Chang, T., and Weisman, R.N. 1990. Predicting incipient fluidization of fine sands in unbounded domains. J.Hydr.Engrg.,ASCE, 116(12), 1454-1467.

Lindley, J.W., and Lennon, G.P. 1991. Finite Difference Approach to Verify Hydraulic Gradients During Fluidization of Fine Sands in Unbounded Domains. Imbt Hydraulic Lab Report No. IHL-136-91, Lehigh University, Bethlehem, PA.

McDonald, M.G., and Harbaugh, A.W. 1988. Techniques of Water-Resources; Investigations of the United States Geological Survey: Chapter A1, A Modular Three-Dimensional Finite-Difference Ground-Water Flow Model. U.S. Geological Survey, Washington.

Roberts, E.W., Weisman, R.N., and Lennon, G.P. 1986. Fluidization of granular media in unbounded two-dimensional domains: An experimental study. Imbt Hydraulics Lab Report No. IHL-109-86, Lehigh Univ., Bethlehem, PA.